Published in final edited form as:
Eur J Neurosci. 2010 March ; 31(6): 978–993. doi:10.1111/j.1460-9568.2010.07133.x.

Biochemical and functional properties of distinct nicotinic acetylcholine receptors in the superior cervical ganglion of mice with targeted deletions of nAChR subunit genes

Reinhard David[1], **Anna Ciuraszkiewicz**[1], **Xenia Simeone**[1], **Avi Orr-Urtreger**[2], **Roger L. Papke**[3], **J. Michael McIntosh**[4], **Sigismund Huck**[1], and **Petra Scholze**[1]

[1]Department of Biochemistry and Molecular Biology, Center for Brain Research, Medical University of Vienna, Spitalgasse 4, A-1090 Vienna, Austria

[2]Genetic Institute, Tel-Aviv Sourasky Medical Center and Sackler School of Medicine, Tel Aviv University, 6 Weizmann Street, Tel Aviv 64239, Israel

[3]Department of Pharmacology and Therapeutics, University of Florida School of Medicine, Gainesville, Florida 32610, USA

[4]Departments of Psychiatry and Biology, University of Utah, 257 S 1400 E, Salt Lake City UT 84112, USA

Abstract

Nicotinic acetylcholine receptors (nAChR) mediate fast synaptic transmission in ganglia of the autonomic nervous system. Here, we have determined the subunit composition of hetero-pentameric nAChRs in the mouse superior cervical ganglion (SCG), the function of distinct receptors (obtained by deletions of nAChR subunit genes), and mechanisms at the level of nAChRs that might compensate for the loss of subunits. As shown by immunoprecipitation and Western blots, wild type (WT) mice expressed (%): α3β4 (55), α3β4α5 (24), and α3β4β2 (21) nAChRs. nAChRs in β4 knockout (KO) mice were reduced to less than 15 % of controls and no longer contained the α5 subunit. Compound action potentials, recorded from the postganglionic (internal carotid) nerve and induced by preganglionic nerve stimulation, did not differ between α5β4 KO and WT, suggesting that the reduced number of receptors in the KO did not impair transganglionic transmission. Deletions of α5 or β2 did not affect the overall number of receptors and we found no evidence that the two subunits substitute for each other. In addition, dual KOs allowed us to study the functional properties of distinct α3β4 and α3β2 receptors that have previously only been investigated in heterologous expression systems. The two receptors strikingly differed in the decay of macroscopic currents, the efficacy of cytisine, and their responses to the α-conotoxins AuIB and MII. Our data - based on biochemical and functional experiments and several mouse KO models - clarifies and significantly extends previous observations on the function of nAChRs in heterologous system and the SCG.

Keywords

Acetylcholine receptor [AChR]; subunit composition; immunoprecipitation; knockout; patch clamp

Corresponding author: Petra Scholze, Department of Biochemistry and Molecular Biology, Center for Brain Research, Medical University of Vienna, Spitalgasse 4, A-1090 Vienna, Austria Phone: +43-1-4277 62873 FAX: +43-1-4277 62879 Petra.Scholze@meduniwien.ac.at.

Europe PMC Funders Author Manuscripts

Introduction

In vertebrates, the autonomic nervous system (ANS) maintains homeostasis under changing physiological demands (De Biasi, 2002). Within ganglia, neurons arising in the brainstem and spinal cord form connections with postganglionic neurons that send their axons to visceral and vascular targets. Mechanisms of ganglionic transmission have been extensively studied in the superior cervical ganglion (SCG), a paravertebral ganglion at the cranial end of the sympathetic chain (Alkadhi *et al.*, 2005a). As the main mediators of fast synaptic transmission in ganglia, neuronal nicotinic acetylcholine receptors (nAChR) play a key role in ganglionic information processing and transfer (De Biasi, 2002).

nAChRs occur as homo- or hetero-pentamers (McGehee & Role, 1995; Corringer *et al.*, 2000; Brejc *et al.*, 2001). In the SCG, the homo-pentameric receptors are made of the α7 subunit, whereas the hetero-pentameric receptors contain the subunits α3, α5, β2, and β4 (Mandelzys *et al.*, 1995; McGehee & Role, 1995; Wang *et al.*, 2002b; Mao *et al.*, 2006; Putz *et al.*, 2008) which might assemble into a variety of receptors of distinct functional properties (McGehee & Role, 1995).

Unfortunately, a great deal of work so far has been done in heterologous expression systems. The disadvantages of such systems include: the effect they might have on the properties of receptors (Lewis *et al.*, 1997), which has lead to conflicting observations and also complicates conclusions concerning the nature of native receptors; the absence of chaperones (Millar, 2008); the relative (and sometimes arbitrary) amounts of mRNA used for transfection (Zwart & Vijverberg, 1998); lowered temperature as required when working with *Xenopus* oocytes (Nelson *et al.*, 2003); diversities of N-glycosylation (Sivilotti *et al.*, 1997); and second messengers that may also be involved in the assembling process (Pollock *et al.*, 2009). Cell-specific mechanisms of nAChR expression have recently been summarized in a topical review (Albuquerque *et al.*, 2009).

The subunit composition and functional properties of nAChRs in dopaminergic neurons have previously been investigated by combining immunoprecipitation, patch clamp, [^{3}H]-dopamine release, and mouse KO models (Champtiaux *et al.*, 2003). However, due to the presence of the subunits α4, α5, α6, β2, β3, and β4, nAChRs in dopaminergic neurons show considerable complexity and occur at mixed populations both at somata and dopaminergic projections (Champtiaux *et al.*, 2003). By taking a similar approach we established the types of hetero-pentameric nAChRs occurring naturally in the wild type (WT) mouse SCG. Using appropriate KO models we could investigate SCG neurons expressing either simple α3β4 or α3β2 receptors, or neurons containing α3β4β2 or α3β4α5, in addition to α3β4 nAChRs. We analysed the functional properties of these receptors, whether a missing subunit would be compensated for at the receptor level, and what effect this might have on transganglionic transmission in the SCG.

Methods

Animals and acute preparation of ganglia

Experiments were performed on wild type C57Bl/6 (WT) mice, and on mice with deletions of the nAChR subunit genes α7 (Orr-Urtreger *et al.*, 1997), α5 (Wang *et al.*, 2002a), β2 (Picciotto *et al.*, 1995), β4 (Kedmi *et al.*, 2004), and α5β4 (Kedmi *et al.*, 2004). β2 KO mice were generously provided by J.-P. Changeux (Pasteur Institute, Paris). α7 KO mice were purchased from Jackson Laboratory. Double KO mice lacking both α5 and β2 were generated by crossing the two single KO lines. α5α7β2-triple KO mice were obtained by crossing α5β2-double with α7-single KO animals. Mice used in this study were backcrossed onto C57Bl/6 background for 6 (β4 and α5β4), 7 (α5, α7) or 12 (β2) generations after germ

line transmission. All animals were kept in thermo stable rooms (21° C) on a light-dark schedule of 10:14 hr in group cages with food and water freely accessible. Animal care and experiments are in accordance with the European Communities Council directive (86/609/EEC) and the Austrian federal law governing animal experimentation (Tierversuchsgesetz TVG 501/1989).

Mostly 18 days old (P18, range 17-19 days) mice were deeply anesthetized with CO_2 and sacrificed by decapitation. Superior cervical ganglia (SCG) were collected in Ca^{2+}-free Tyrode's solution: 150 mM NaCl, 4 mM KCl, 2.0 mM $MgCl_2$, 10 mM glucose, and 10 mM HEPES, pH 7.4. After removal of the Tyrode's solution, ganglia were flash-frozen with liquid nitrogen and stored at −80° C for later use.

Transganglionic transmission

Adult mice of either sex at the age of 4-6 weeks were put under deep CO_2 anesthesia and decapitated while the heart was still beating. The two SCGs with their pre- and postsynaptic nerves attached were removed and kept in oxygenated Locke's solution for the entire experiment. The composition of the Locke's solution was (mM): NaCl 136, KCl 5.6, $CaCl_2$ 2.2, $MgCl_2$ 1.2, NaH_2PO_4 1.2, $NaHCO_3$ 20, and dextrose 8, continuously bubbled with 95 % O_2 - 5% CO_2 (pH 7.2-7.4). Preganglionic nerves were supramaximally stimulated with a suction electrode connected to an ISO-Flex stimulus isolator / Master 8 pulse generator (A.M.P.I., Jerusalem) at 0.5Hz with a pulse width of 50 μsec. Compound action potentials of the postganglionic (internal carotid) nerve were measured at room temperature with a suction electrode and a differential amplifier (Meta Metrics Corporation, Carlisle, MA). The amplitudes of 20 compound action potentials were averaged for a comparison of the three different genotypes WT, α5β4 KO, and α5β2 KO.

Cell culture of SCG neurons

SCGs were dissected from 5 to 6 day-old (P5 to P6) mouse pups killed by decapitation. The use of enzymes, the trituration protocol, and the culture conditions were similar to published procedures (Fischer *et al.*, 2005), except that 10 % fetal calf serum (FCS, Sigma F7524) was added to the culture medium for trituration. We seed 10 000 cells into 8 mm glass rings in order to confine the cells to the center of 35 mm tissue culture dishes (Nunc). Cells were routinely cultured at 5 % CO_2 and 36.5° C for 3-5 days before use. Unless otherwise mentioned, cells from α5β4 KO mice were kept in the presence of 100 μM nicotine, added to cultures after one day *in vitro* and removed at least 2 hours before the recordings.

Membrane-Preparation

We homogenize tissue (cerebellum, SCG or HEK cells) in ice-cold homogenization buffer (10 mM HEPES, 1 mM EDTA, 300 mM sucrose, pH = 7.5, supplemented with 1 complete mini protease inhibitor cocktail tablet (Roche) per 10 ml buffer). Exactly three pulses of 5 seconds duration with the power level set to 30% were delivered by an ultrasonic homogenizer (Bandelin Sonopuls UW2200). We took great care to avoid excessive foam formation by precise positioning of the MS73 sonotrode tip. Following centrifugation of the homogenate for 30 min at 4° C and 50 000 g, the pellet was re-suspended in homogenization buffer without sucrose, incubated on ice for 30 minutes, and centrifuged again for 30 min at 50 000 g. Membrane preparations were always used the same day.

[^{3}H]-epibatidine membrane binding

Membranes prepared as described above were homogenized in 50 mM Tris HCl pH = 7.4. Membranes of 2-4 SCG (equivalent to 10-20 μg membrane protein) per reaction tube were incubated with [^{3}H]-epibatidine ([5,6.bicycloheptyl-^{3}H](+/−)epibatidine, NEN-PerkinElmer)

in a final volume of 200 μl for 2 hours at room temperature. Nonspecific binding was determined by the presence of 300 μM nicotine and subtracted from total binding in order to obtain specific binding. Receptors were separated from free ligand by vacuum filtration over GF/B glass-microfiber filters (Whatman, Schleicher & Schuell) that were pre-wet with 0.5 % polyethyleneimine (Sigma P3143). Filters were submerged in scintillation cocktail, and their radioactive contents were determined by liquid scintillation counting.

Generation and purification of antibodies

All antibodies were targeted against the cytoplasmic loop region of mouse nAChR subunits: anti-α3 against amino acids (aa) 354-467; anti-α4 against aa 365-446; anti-α5 against aa 333-389; anti-β2 against aa 353-422; and anti-β4 against aa 350-426. Rabbits were immunized with a maltose binding fusion protein linked to the corresponding loop peptide. The antibodies were purified by using the corresponding glutathione S-transferase fusion protein coupled to Affi-Gel 10 (Bio-Rad).

Immunoprecipitation of [^{3}H]-epibatidine labeled receptors

Receptors were solubilized by re-suspending membrane preparations (described above) in 2 % Triton X-100 lysis buffer: 50 mM Tris-HCl pH = 7.5, 150 mM NaCl, 2 % Triton X-100, supplemented with one complete mini protease inhibitor cocktail tablet (Roche) per 10 ml buffer. Following two ultrasound pulses of 5 seconds duration at 30 % energy level, samples were left for 2 hours at 4° C and thereafter centrifuged at 16 000 g for 15 min at 4° C. 150 μl clear supernatant containing the membranes of 3 SCG (WT, α5 KO, β2 KO, α5β2 KO), or 10 SCG (β4 KO, α5β4 KO), respectively, were incubated with 20 μl 1 nM [^{3}H]-epibatidine and 7 μg antibody in 10-15 μl phosphate-buffered saline (PBS: 10 mM Na_2HPO_4, 1.8 mM KH_2PO_4, 2.7 mM KCl, 140 mM NaCl, pH = 7.4) on a shaking platform at 4° C over night. On average, we obtain 1-1.5 μg solubilized protein from our ganglia. Unspecific binding was determined by adding 300 μM nicotine to half of the samples.

Heat-killed, formalin-fixed Staphylococcus aureus cells carrying protein A (Standardized Pansorbin-cells, Calbiochem) were centrifuged at 2300 g for 5 min at 4° C. The pellets were washed twice with IP-High (50 mM Tris-HCl pH = 8.3, 600 mM NaCl, 1 mM EDTA, 0.5 % Triton X-100), once in IP-Low (50 mM Tris-HCl pH = 8.0, 150 mM NaCl, 1 mM EDTA, 0.2 % Triton X-100), and re-suspended with IP-Low. 20 μl of this suspension of Pansorbin cells were added to the above mentioned cocktail containing the antibody, solubilized receptors, and [^{3}H]-epibatidine for 2 hours at 4° C on a shaking platform. Samples were centrifuged at 2 300 g for 5 min at 4° C and washed twice with IP-High and once with IP-Low at 2 300 g for 1 min at 4°C. Pellets were re-suspended in 200 μl 1 N NaOH and subjected to liquid scintillation counting.

Quantification of protein contents in membrane preparations and lysates

All protein quantifications were performed using the Micro BCA Protein Assay Reagent Kit (Pierce) following the manufacturer's instructions.

Immunoprecipitation of receptors followed by Western blot

For each sample of lysed receptors, 20 μl M-20 sheep anti-rabbit immunoglobulin G Dynabeads (Invitrogen) were washed three times and re-suspended in 150 μl 2 % Triton X-100 lysis buffer. Triton X-100 lysates of SCG membranes were prepared as described above for radioligand immunoprecipitation. Lysates of 15 SCG (corresponding to 15-20 μg lysate protein) were incubated with 150 μl pre-washed Dynabeads and 7 μg antibody on a shaking platform at 4° C over night. Dynabeads were pelleted using a magnet supplied by

the manufacturer, washed 3 times in 500 μl PBS, re-suspended in 20 μl SDS-PAGE sample buffer, and heated to 65° C for 15 min.

SDS-PAGE, Western blot and chemoluminescence detection

20 μl of tissue lysates were diluted in reducing sample buffer to a final concentration of 62.5 mM Tris/HCl pH = 6.8; 5 % α-mercaptoethanol, 2 % SDS; 10 % glycerol, and 0.01 % PyroninY. These samples, or the 20 μl samples released from Dynabeads described above, were denatured for 15 min at 65° C and separated on 10% SDS gels using a Tris-glycine buffer system (25 mM Tris, 192 mM glycine, 0.1 % SDS). The size of proteins was determined by mixing 0.3 μl MagicMark XP Western Protein Standard (Invitrogen) with 10 μl SeeBlue Plus2 Pre-Stained Standard (Invitrogen). Proteins were tank-blotted onto pre-wetted polyvinylidene fluoride membranes (Immobilon-P PVDF-Membrane, Millipore IPVH00010). After blocking with blocking buffer (5 % nonfat dry milk powder in PBS, 0.1 % Tween 20) over night at 4° C, the membranes were incubated with 1 μg/ml primary antibody in blocking buffer for 2 hours at room temperature.

Membranes were then washed extensively with washing buffer (1.5 % nonfat dry milk powder in PBS including 0.1 % Tween 20) and incubated for 1 hour at room temperature with peroxidase-conjugated mouse anti-rabbit light chain-specific secondary antibody (Jackson ImmunoResearch Laboratories), diluted 1:10 000 in washing buffer. Following another extensive washing step, membranes were submerged in Immobilon Western Chemiluminescent HRP substrate (Millipore WBKLS0500) for 5 minutes and sealed in foil. Signals were documented with a Fluor-S Max Multi-Imager (BioRad).

Patch clamp recordings

We used standard techniques for perforated patch clamp recordings as previously described (Fischer *et al.*, 2005). The internal (pipette) solution consisted of 75 mM K_2SO_4, 55 mM KCl, 8.0 mM $MgCl_2$ and 10 mM HEPES, adjusted to pH = 7.3 with KOH. Access to cells was achieved by including 200 μg/ml amphotericin B (Rae *et al.*, 1991). Cells were voltage-clamped at −70 mV. For recording and signal processing we used an Axopatch 200B patch clamp amplifier, a Digidata 1320A data acquisition system, and the pCLAMP 10 software (all from Molecular Devices).

Application of substances

Substances were dissolved in external (bathing) solution consisting of: 120 mM NaCl, 3.0 mM KCl, 2.0 mM $CaCl_2$, 2.0 mM $MgCl_2$, 20 mM glucose, 10 mM HEPES, and 0.5 μM tetrodotoxin (TTX, Latoxan), adjusted to pH = 7.3 with NaOH. 0.1 mg/ml bovine serum albumin was added to solutions when probing the effects of the α-conotoxins AuIB and MII. In order to block muscarinic responses, ACh was always combined with 0.1 μM atropine. The substances were applied by means of a DAD-12 solenoid-controlled superfusion system (ALA Scientific Instruments) with a tip diameter of 100 μm and reservoirs set to a pressure of 250 mm Hg. With the tip of the superfusion placed 120 μm above our cells we reach 75 % of the final concentration of solutions within 35 msec. This is considerably slower than the rapid application system used by others (full concentration reached within 5 msec) to record the currents carried by the fast desensitizing splice variant α7-1 of the α7 nAChR (Zhang *et al.*, 1994; Severance *et al.*, 2004). By comparing their rapid application with a conventional but slower puffer pipette, these authors concluded that the high speed of the superfusion is a prerequisite for the detection of currents in response to α7-1 activation in chick ciliary ganglion neurons (Zhang *et al.*, 1994). Upon probing our DAD-12 superfusion setup on freshly dissociated embryonic day 14 (E14) chick ciliary ganglion neurons we recorded rapidly decaying α7-1 currents (supplemental Fig. 2), though of a lesser amplitude than has been reported (Zhang *et al.*, 1994). While response kinetics of α7-1 receptors are

most affected, the limited speed of our superfusion system will also just partly disclose the quality of α3β2 receptor activation. Relatively slowly desensitizing receptors such as α3β4 will be least affected.

Reagents

General chemical reagents were from Merck-VWR-Jencons. Substances not particularly mentioned were from Sigma-Aldrich. PNU-120596 (# 2498) and cytisine (# 1390) were from Tocris.

Data analysis

Unless otherwise noted, all data are presented as means ± SEM. Statistical analyses and curve fitting were done with GraphPad Prism version 4.0 (GraphPad Software). Data points for the binding of [^{3}H]-epibatidine were fitted to a hyperbolic curve based on a one-site model. Concentration-response measurements of drug effects were fitted to sigmoidal curves using the logistic equation:

$$E_{(x)}=E_{max} * x^p / (x^p+EC_{50})$$

Where $E_{(x)}$ is the response to a certain drug concentration; x the arithmetic dose; E_{max} the maximal response; EC_{50} the dose that gives half-maximal response; and p a slope factor, which is numerically identical to the Hill coefficient. Agonist low-concentration potency ratios were calculated as previously described (Fischer *et al.*, 2005), except that we now use the curve fitting routine of GraphPad Prism with the constraints of a shared slope and with maximal responses fixed to values deduced from parallel experiments. Student's *t*-test, one-way analysis of variance (ANOVA), or non-parametric Mann-Whitney or Wilcoxon tests were performed when appropriate. The decay of currents in the presence of an agonist was fitted to two standard exponentials curves using the Chebyshev algorithm included in the Clampfit software (Molecular Devices).

Results

Membrane binding of [^{3}H]-epibatidine to nicotinic receptors is significantly reduced in the SCG of β4 KO mice

We first determined the kinetics of [^{3}H]-epibatidine binding to SCG membrane homogenates of 17 to 19 day-old (mostly postnatal P18) WT mice. The binding was saturable with a KD of 150.7 ± 25.6 pM and a Bmax 345.8 ± 25.6 fmol/mg protein (Fig. 1A; n = 4 different experiments). Binding is maximal at 1 nM epibatidine, the concentration used thereafter for all further assessments of the total number of hetero-oligomeric nAChR binding sites. Epibatidine binds with high affinity in the picomolar range to hetero-oligomeric nAChRs (Houghtling *et al.*, 1995), and with much lower affinity (greatly in excess to 1 nM) to α7 homo-oligomeric nAChRs (Sharples *et al.*, 2000). In keeping with these reports we did not find significantly reduced [^{3}H]-epibatidine binding when using SCG membranes from α5α7β2 KO mice (Fig. 1B).

Figure 1B compares the specific [^{3}H]-epibatidine binding in membrane homogenates prepared from SCGs of WT and 6 different KO mouse lines. Note that the number of receptors is significantly reduced not only in α5β4-double, but also in β4-single KO mice (to 8 % and 13 % of control, respectively, Fig. 1B). None of the other genotypes, including the α5α7β2-triple KO, showed a reduced number of [^{3}H]-epibatidine binding sites (genotypes compared by one-way ANOVA, $F = 35.46$, $P < 0.0001$, followed by Dunnett's

post-hoc multiple comparison test referenced to wild-type, $^{**}P < 0.01$ for β4-single and α5β4-double KO, all other $P > 0.05$).

Antibodies for immunoprecipitation assays

Subunit-specific antibodies are essential prerequisites for the analysis of the subunit composition of nAChR subtypes. We thus generated antibodies directed against the subunits α3, α4, α5, β2 and β4. With the exception of anti-α3, all antibodies were tested not only on native receptors of WT mice (positive controls) but also on neuronal materials of appropriate KO animals (negative controls). Such rigorous controls have turned out essential in order to exclude false-positive results (Gotti *et al.*, 2006; Moser *et al.*, 2007). A detailed characterization of these antibodies is provided in the supplemental Fig. 1. Note that our antibodies are not only highly specific but also immunoprecipitate with excellent efficacy, as shown by comparison with polyethyleneglycol precipitation (supplemental Fig. 1). Polyethyleneglycol precipitates all proteins in solution and thus serves as a reference for 100 % of precipitated, radioligand-labeled receptors.

Each neuronal-type hetero-oligomeric receptor must contain either β2 and/or a β4 (Champtiaux & Changeux, 2004). We judged the overall number of [^{3}H]-epibatidine binding sites by immunoprecipitation with anti-β2 and anti-β4 antibodies used in conjunction, and deduced the relative occurrence of receptors made of the subunits α3, α4, α5, β2 and β4 by precipitations with appropriate subunit-specific antibodies in isolation. However, the use of either anti-β4 or anti-β2 in β2 and β4 KO animals, respectively, will suffice to immunoprecipitate all hetero-oligomeric receptors in the SCG of these mice. Anti-α3 antibodies consistently immunoprecipitated the same number of receptors as either anti-β4, anti-β2 (in their complementary KO), or the combined use of the two antibodies (Fig. 2), indicating that all receptors in the SCG of P18 mice contain α3. It is worth noting that α4-containing receptors are absent in the SCG not only of P18 mice (Fig. 2A-D) but also of adult rats (Mao *et al.*, 2006).

Receptors containing the accessory subunits α5 and β2

As shown in Fig. 2A, 100 % of receptors in the SCG of WT animals contain the subunits α3 and β4. Anti-α5 as well as anti-β2 antibodies precipitated approximately 20 % of all receptors. These observations allow, in principle, for 4 types of receptors: α3β4, α3β4α5, α3β4β2, and α3β4α5β2. To investigate whether all these combinations are present in the mouse SCG we immunoprecipitated receptors using the anti-α5 and anti-β2 antibodies alone and in combination (Fig. 3C). The algebraic sum (429 ± 93 fmol/mg protein) did not differ significantly from results when the two antibodies were used together (402 ± 98 fmol/mg protein; $P > 0.05$; one-way ANOVA, followed by Dunnett's *post-hoc* multiple comparison test referenced to the combined use of both antibodies). In contrast, each antibody alone (anti-α5: 250 ± 79 fmol [^{3}H]-epibatidine per mg protein; anti-β2: 179 ± 15 fmol per mg protein) precipitated significantly less [^{3}H]-epibatidine receptor binding sites than the combination of both antibodies ($^{**}P < 0.01$; one-way ANOVA, followed by Dunnett's *post-hoc* multiple comparison test referenced to the combined use of both antibodies). These data suggest that α5 and β2 are not co-expressed in the same receptor, and that only 3 types of receptors are present in the SCG of P18 WT mice: α3β4 (55 %), α3β4α5 (24 %), and α3β4β2 (21 %, Fig. 2A).

Further evidence that α5 does not co-assemble with β2

Western blots provided further evidence that α5 does not co-assemble into the same receptor with β2. Hence, immunoprecipitation with anti-α3, but not with anti-α5, resulted in a band of approximately 52 kD when probed with our anti-β2 antibody (Fig. 3D). Importantly, the anti-β2 antibody showed no signal in Western blots from whole brain or SCG extracts of β2

KO animals (Fig. 3D). In contrast, our anti-β4 antibody detected a band of approximately 56 kD when solubilized receptors were immunoprecipitated with either anti-α3 or anti-α5 antibodies (Fig. 3E). These observations provide good evidence that α5 co-assembles with the β4, but not with the β2 subunit in the SCG of WT animals. Furthermore, α5 could not even be forced into co-assembling with β2 in our β4-single KO mouse model (Fig. 2D; Fig. 3A). Hence, only a single type of α3β2 hetero-oligomeric receptors was found in the SCG not only in α5β4-double (supplemental Fig. 1), but also in β4-single KO mice (Fig. 2D).

The subunits α5 and β2 are tightly regulated in the SCG

Deletion of the α5 subunit did not affect the number of β2-containing receptors (Fig. 3B), indicating that β2 subunits otherwise unused do not take the place of α5 (in this case the number of β2-containing receptors should rise from about 20 % to 40 %). In fact, the number of β2-containing receptors remained stable even when the β4 subunit was deleted (Fig. 3B). Since only about 20 % of receptors in the SCG of WT animals contain the β2 subunit, this caused a major reduction of the overall number of [^{3}H]-epibatidine receptor binding sites (Fig. 1B; Fig. 2D).

We also found the α5 subunit is tightly regulated. When comparing WT and β2 KO animals we saw no significant difference in the number of α5-containing receptors, indicating that α5 does not substitute for the loss of β2 (Fig. 3A).

Functional α7 receptors in SCG cell cultures

Once we had established the types of receptors encountered in the SCG we preceded with their functional characterization by patch clamp recordings. We focused on two hetero-oligomeric receptors consisting of the subunits α3β2 and α3β4, since the properties of such “pure” receptors have so far only been investigated in heterologous expression systems.

To exclude contributions from α7 homo-oligomeric nAChRs we followed published protocols that detect currents due to the activation of α7. SCG neurons freshly dissociated from 10-14 days old rats have two types of currents in response to the activation of two splicing variants of the α7 gene: One of quite low amplitude (α7-1, currents in the pA range) with extremely rapid, and a second (α7-2, currents in the nA range) with relatively slow desensitization kinetics (Cuevas *et al.*, 2000; Severance *et al.*, 2004). Currents due to α7-2 activation by 500 μM ACh are inhibited in a reversible manner by both α-bungarotoxin and methyllycaconitine (MLA) (Cuevas *et al.*, 2000). We did not see any inhibition of these currents by MLA (Sigma M168), suggesting that this component, if present in the P5-P7 mouse SCG, is lost when cells are maintained in culture (Fig. 4A2; Fig. 4B2).

We also probed our cultures for rapidly desensitizing α7 receptors with choline, a full agonist for α7 receptors (Papke *et al.*, 1996; Cuevas *et al.*, 2000). Choline concentrations ranging from 3-30 mM induced negligible currents in cultured SCG neurons obtained from α5β4 KO animals (Fig. 4A1, A2), but slowly decaying currents of considerable amplitude in our α5β2 KO preparations (Fig. 4B1, B2). The slowly desensitizing currents were due to the sole activation of α3β4 without any contribution by α7 receptors, since they were also seen in our α5α7β2-triple KO mice (Fig. 4C1, C2).

We never experienced a rapidly decaying component as seen in freshly dissociated rat SCG neurons (Cuevas *et al.*, 2000). However, choline effects were boosted to a variable extent by the positive allosteric α7 modulator PNU-120596 (Hurst *et al.*, 2005), and this effect was reversed by a 2 min pre-treatment with 5 nM MLA (Fig. 4). Since α3β2 receptors were hardly activated by choline, the effects of PNU-120596 were more obvious in SCG neurons of α5β4 than of α5β2 KO mice (compare Fig 4. A2 with B2). Nonetheless, net

PNU-120596 effects (seen by subtracting peak currents in the absence of the α7 modulator from currents in the presence of PNU-120596) were significantly larger in α5β2 KO compared to α5β4 KO animals ($P = 0.0023$, Mann-Whitney comparison of data shown in Fig. 4A3 and 4B3). PNU-120596 had no effect in the absence of choline, nor did it enhance choline-induced currents in α5α7β2-triple KO mice subunit (Fig. 4C1, C2), indicating that the effect of the modulator is indeed specific for α7. The small enhancement of ACh-induced currents by PNU-120596 in α5β2 KO animals (Fig. 4B2) seems unrelated to an effect on α7 receptors, since it is also seen in our α5α7β2-triple KO mice (Fig. 4C2).

We also tested 10 μM PNU-120596 on freshly dissociated E14 chick ciliary ganglion neurons, a preparation renowned for its high density of rapidly inactivating α7 receptors (Zhang *et al.*, 1994). Peak currents in response to 10 mM choline (40.4 ± 3.8 pA/pF, n = 15) increased to 1688 ± 204 pA/pF in the presence of PNU-120596 (supplemental Fig. 2). In view of this observation, the effect of PNU-120596 in cultured SCG neurons appears unimpressive (median values of 4.29 and 9.90 pA/pF for α5β2 and α5β4 KO, respectively; Fig. 4A3, B3). We thus conclude that functional α7-1 receptors are expressed in cultured mouse SCG neurons, but due to their small size are detected by our techniques only in the presence of PNU-120596. It is worth noting that rapidly desensitizing currents due to α7-1 in freshly dissociated rat SCG neurons are significantly smaller (currents in the pA range, Cuevas *et al.*, 2000) than in chick ciliary ganglion neurons (currents in the nA range, Zhang *et al.*, 1994) and thus much more likely missed. Previous attempts to record α-bungarotoxin-sensitive currents in cultured rat SCG neurons have equally failed, in spite of clear [^{125}I]-α-bungarotoxin binding to plasma membrane receptors in intact neurons (De Koninck & Cooper, 1995).

α3β2 receptors in the mouse SCG

In the absence of measurable α7 responses, the currents remaining in our α5β4-double KO mice will be due to just α3β2 receptor activation. Agonist-induced peak currents in cultured SCG neurons taken from α5β4 KO were significantly smaller than from α5β2 KO animals (Table 1, Table 2, compare Figs. 5 and 6). These results are in keeping with our observation of a reduced number of [^{3}H]-epibatidine binding sites in the SCGs of P18 α5β4 KO animals (Fig. 1B) and suggest that not only the total number of receptors but also the number of plasma membrane receptors is reduced in animals lacking the β4 subunit. Culturing neurons from α5β4 KO animals in the presence of 100 μM nicotine increased the currents in response to ACh (Fig. 5C), though effects were clearly less than in HEK tsA201 cells expressing α3β2 (Wang *et al.*, 1998). Nonetheless, we routinely added nicotine to a final concentration of 100 μM after one day *in vitro* to our cultures and removed it at least 2 hours before the recordings.

The most conspicuous, though not unexpected, feature of α3β2 receptors is the rapid decline of macroscopic currents in response to nAChR agonists (Fig. 5A, D), consistent with rapid equilibration of activation and desensitization, favouring the desensitized state of this receptor subtype. When fitted to a double-exponential function, currents induced by 300 μM ACh decay with two time constants of 132 ± 8 (fast, τ_f) and 1129 ± 89 msec (slow, τ_s), respectively (Fig. 5D, Table 2). The rate of fluid exchange of our superfusion system (see Methods) is not fast enough for an accurate determination of concentration-response parameters of such rapidly desensitizing receptors and will cause an underestimation of the slope and of peak currents at high agonist concentrations. Relatively slowly desensitizing receptors such as α3β4 will be less affected.

Notwithstanding this limitation, we can estimate EC_{50} values (Table 1) and thus rank the potencies of agonists for α3β2 receptors. Given the low efficacy of cytisine at α3β2 receptors (about 10% of the maximal currents of 1,1-dimethyl-4-phenylpiperazinium iodide

(DMPP); Table 1, Fig. 5B) we did not construct dose-response curves for this substance, a known partial agonist/antagonist for receptors containing the β2 subunit (Luetje & Patrick, 1991; Papke & Heinemann, 1994; Nelson *et al.*, 2001). Since the α5 subunit does not assemble into α3β2 receptors (Fig. 2D, Fig. 3A), we did not include the analysis of β4-single KO animals in our patch clamp experiments.

α3β4 receptors in the mouse SCG

As documented above, about 55 % of receptors in the SCG of WT animals consist of the subunits α3 and β4, 24 % also contain α5, and 21 % hold β2. Unlike in human IMR-32 cells, where α5 (5 %) and β2 (6 %) contribute little to the overall number of α3β4 receptors (Nelson *et al.*, 2001) we might thus expect more distinct differences in receptor function between WT and α5β2 KO. Indeed, DMPP was more potent than cytisine in the SCG of α5β2 KO mice (Table 1, Fig. 7), whereas the potencies of the two agonists are reversed in WT animals (Fischer *et al.*, 2005). This shift of agonist potencies seems primarily due to the deletion of the α5 subunit, since we observed it as well in α5-single KO mice (Fischer *et al.*, 2005). Though deletions of the subunits α5 and β2 leave just α3β4 receptors in the SCG we noticed two current components when using nicotine as an agonist (apparent as an early “hump” in the current traces at lower concentrations, Fig. 6A2). One explanation of the phenomenon could be the presence of two receptors with an alternate stoichiometry. It has previously been shown that HEK 293 cells permanently transfected with the α4 and the β2 subunits express both 2(α4)3(β2) and 3(α4)2(β2) receptors with different sensitivities to nAChR agonists, in particular ACh (Nelson *et al.*, 2003). By testing the hypothesis that α3β4 receptors, expressed with varied stoichiometry in *Xenopus* oocytes, might also display different pharmacological properties we found decreased potencies of both ACh and nicotine upon enhancing the presence of α3 at the expense of β4 (supplemental Fig. 3). When applied to our observations in the SCG, the first and the second peak could thus be due to the activation of 2(α3)3(β4) and 3(α3)2(β4), respectively. It is worth noting that α3 mRNA exceed β4 levels by about a factor of 2 in the adult mouse SCG (Putz *et al.*, 2008).

α3β4α5 receptors in the mouse SCG

Deletion of the β2 subunit will leave α3β4α5 receptors, in addition to the more numerous α3β4 subunit combination (Fig. 2C). Contrary to α5β2 KO animals, cytisine was more potent than DMPP when the two agonists were used in low concentrations (Fig. 7: potency ratio: 0.76 ± 0.04; significantly different from α5β2 KO: $P < 0.001$, Newman-Keuls multiple comparison test following one-way ANOVA, $F = 28.47$, $P < 0.0001$; see also Fig. 6B). Low-concentration potency ratios were originally introduced to take differences of receptor desensitization at high agonists concentrations into account (Luetje & Patrick, 1991; Covernton *et al.*, 1994). In fact, the potency ratio of cytisine relative to DMPP calculated from responses at the lower end of the concentration-response curves differed significantly from results derived from full concentration-response curves for both genotypes (Fig. 7. One-way ANOVA ($F = 28.47$, $P < 0.0001$), followed by Newman-Keuls multiple comparison test: β2 KO: $P < 0.001$; α5β2 KO: $P < 0.05$ KO). Potency ratios of cytisine relative to DMPP at low concentrations have previously proven sensitive discriminators for receptors containing the subunits α3 and β4 (Fischer *et al.*, 2005).

α3β4α5 expressed in *Xenopus* oocytes differ from α3β4 receptors by macroscopic currents with significantly faster decay time constants (Gerzanich *et al.*, 1998). We tested whether we could see such a difference in the decay of macroscopic currents between β2 KO (leaving α3α5β4 in addition to α3β4 receptors) and α5β2 KO (leaving just α3β4 receptors). However, when fitting the decay of current in response to 300 μM ACh to the sum of two exponential functions we found both the fast (T_f) and the slow time constants (T_s)

unaffected by the presence of ACh. Nonetheless, the amplitude of the slow component increased slightly at the expense of the fast component when α5 was absent (Table 2).

Effects of the α-conotoxins AuIB and MII

Our double KO mice enabled us to investigate the effects of the two α-conotoxins AuIB and MII on "pure" α3β4 and α3β2 receptors in SCG neurons and to compare these results with observations in WT animals (Fig. 8). α-Conotoxin AuIB rapidly and reversibly inhibited α3β4 receptors (Fig. 8A2, A3), with about one order of potency less than rat α3β4 receptors expressed in *Xenopus* oocytes (Luo *et al.*, 1998). In comparison with nAChRs in WT SCG (Fig. 8B2, B3), the currents induced by 300 μM ACh were somewhat more reduced in the α5β2 KO (Fig. 8B3: AuIB at 5 μM: α5β2 KO: 55.2 ± 2.9 % of control, n = 8 cells; WT: 63 ± 2.4 %, n = 14 cells; $P = 0.0483$, Student's *t*-test; AuIB at 10 μM: α5β2 KO: 34.0 ± 2.5 %, n = 7 cells; WT: 43.0 ± 3.0 %, n = 8 cells; $P = 0.0414$, Student's *t*-test), suggesting that co-assembling of the subunits α5 and/or β2 into α3β4 nAChRs interferes with the effect of the toxin. 5 μM α-conotoxin AuIB did not affect the currents induced in SCG neurons of α5β4 KO mice (Fig. 8C1).

α-Conotoxin MII, on the other hand, rapidly inhibited α3β2 receptors with high potency (Fig. 8C2). Consistent with previous observations (Cartier *et al.*, 1996), recovery from inhibition was slow and incomplete (Fig. 8C3). 100 nM of α-conotoxin MII did not affect α3β4 nAChRs (Fig. 8A1), but slightly reduced currents in response to 300 μM ACh in SCG neurons taken from WT animals (to 98.2 % of control peak currents after 250 sec of toxin application, $P = 0.0498$, one sample Student's *t*-test with reference to a hypothetical 100 %, n = 13 cells, Fig. 8B1). These observations are in keeping with the reported high affinity and selectivity of α-conotoxin MII for α3β2 receptors (Cartier *et al.*, 1996) and suggest that few, if any, β2 subunits form an interface with α3 in WT SCG neurons. Importantly, we did not encounter SCG neurons of WT mice with currents that were particular sensitive to the toxin. This is in contrast to α3-containing receptors in chick ciliary ganglion neurons that are highly susceptible to 300 nM α-conotoxin MII (Nai *et al.*, 2003).

Transganglionic neurotransmission in WT, α5β2 KO, and α5β4 KO animals

We measured postganglionic compound action potentials of ganglia dissected from WT, α5β2 KO, and α5β4 KO animals and found no significant differences in the amplitudes of the three preparations (Fig. 9). The experiments indicate that supramaximal stimulation of the preganglionic nerve will activate the same number of postganglionic nerves in the 3 genotypes. Hence, synaptic transmission is maintained despite of a significantly reduced overall number of nAChRs in the α5β4 KO animals.

Discussion

With self-generated, subunit-specific antibodies we have established 3 types of hetero-pentameric receptors in the WT mouse SCG: α3β4 (55 %), α3β4α5 (24 %), and α3β4β2 (21 %). Hence, all receptors in the SCG contain α3 and β4, and the subunits α5 and β2 are never co-assembled into the same receptor. Furthermore, targeted deletion of β4 also removed all α5-containing receptors, indicating that even under these stringent conditions, the α5 subunit could not be forced into assembly with β2. β4-single KO mice - just as α5β4-double KO - thus express only α3β2 hetero-pentameric receptors.

Mice lacking the β4 subunit had significantly reduced [^{3}H]-epibatidine binding and whole cell currents, indicating less overall and cytoplasmic membrane nAChRs in this genotype. Nonetheless, the amplitude of compound action potentials recorded from postganglionic nerves did not differ significantly from WT animals.

Choline, a proposed α7-specific agonist, induced sizeable currents in SCG neurons from both α5β2-double and α5β2α7-triple KO mice, indicating that these currents are due to the activation of α3β4 receptors. In keeping with this conclusion, the currents in response to choline were negligible in α5β4-double KO animals. However, choline in the presence of the positive α7-specific modulator PNU-120596 induced currents (of quite variable amplitudes) in the α5β4-double KO and enhanced the currents in SCG neurons of α5β2-double KO mice.

"Pure" α3β4 nAChRs were activated by the nicotinic receptor agonists with a rank order of potency DMPP > nicotine = cytisine > ACh. This rank order was similar for α3β2 receptors, though cytisine was a poor agonist in the α5β4 KO. Furthermore, α3β4 and α3β2 receptors differed remarkably in the decay of macroscopic currents and their responses to the α-conotoxins AuIB and MII. In contrast with previous observations in *Xenopus* oocytes (Wang *et al.*, 1996; Gerzanich *et al.*, 1998), we did not see an effect of the α5 subunit on the decay of macroscopic currents after α3β4 receptor activation.

nAChRs in the rodent SCG

We found α3β4, α3β4β2, and α3β4α5 nAChRs in the mouse SCG that are virtually identical to the rat by their subunit composition, by the frequency of their occurrence, as well as by overall [^{3}H]-epibatidine binding (480 fmol/mg protein, Mao *et al.*, 2006). Likewise, the KD of [^{3}H]-epibatidine binding in our membrane preparation (150.7 ± 25.6 pmol/l) compares well with previous findings in the adult (intact) mouse SCG (137 pmol/l, Del Signore *et al.*, 2002). This close similarity between the two species is noteworthy, as we have previously observed major differences of nAChR function at noradrenergic nerve terminals in the rat and mouse hippocampus (Scholze *et al.*, 2007).

nAChRs remaining after deletions of distinct subunits

In the brain, β2-containing receptors greatly outnumber receptors that contain β4 (McGehee & Role, 1995; Albuquerque *et al.*, 2009), and in most brain regions, targeted deletion of the β2 subunit virtually abolishes [^{3}H]-epibatidine binding and receptor autoradiography (Zoli *et al.*, 1998) due to the absence of a β subunit required to form functional nAChRs (Champtiaux & Changeux, 2004). Although both β subunits are expressed in the WT mouse SCG, we find the overall number of receptors in the β4 KO reduced by > 85 % (to about the expression level of β2 in WT mice), indicating that β2 does not substitute for an absent β4 subunit. These results significantly extend our previous observation that β2 expression is tightly regulated (Putz *et al.*, 2008) and thus limits the formation of receptors in the SCG. Interestingly, the deletion of β4 also removed all receptors containing the α5 subunit, implying that α5 under no circumstances could be forced into co-assembling with α3β2 in the mouse SCG. α3β2α5 have been expressed in *Xenopus* oocytes (Wang *et al.*, 1996; Gerzanich *et al.*, 1998) and in HEK293 cells (Nelson *et al.*, 2001), and may occur in the rat superior colliculus (see Gotti *et al.*, 2006). In contrast to β4-single and the α5β4-double KO, deletions of either α5 or β2 had no effect on the overall number of receptors. Furthermore, the two subunits did not substitute for each other when one was deleted.

Functional characterization of hetero-pentameric nAChRs in the mouse SCG – lessons from KO

We and many others have used nAChR agonists for a "pharmacological fingerprinting" of receptors (e. g. Colquhoun & Patrick, 1997b; Kristufek *et al.*, 1999; Fischer *et al.*, 2005; Gotti *et al.*, 2006). Our current patch clamp experiments show that DMPP activates somatic α3β4 receptors (in the SCG of α5β2-double KO mice) somewhat more potently than cytisine (low-concentration potency ratio cytisine/DMPP: 1.23, Fig. 6B1, Fig. 7). These data compare well with rα3β4 receptors expressed in HEK cells (potency ratio: 1.47, Wong *et*

al., 1995) and human α3β4 receptors in *Xenopus* oocytes (potency ratio: 4, Chavez-Noriega *et al.*, 1997) or HEK cells (potency ratio: 1.29, Nelson *et al.*, 2001). Other reports show cytisine more potent than DMPP for rα3β4 receptors expressed in *Xenopus* oocytes (Luetje & Patrick, 1991; Covernton *et al.*, 1994) or in L-929 fibroblasts (Lewis *et al.*, 1997).

Removal of just the β2 subunit leaves α3β4 receptors in the SCG with and without α5 that are overall more sensitive to cytisine than to DMPP (low-concentration potency ratio cytisine/DMPP: 0.76, Fig. 6B2, Fig. 7). An increased potency of cytisine has previously been observed when α5 co-assembled with hα3β4 receptors in *Xenopus* oocytes (Gerzanich *et al.*, 1998). We can, however, not confirm that the presence of α5 confers enhanced desensitization as well as increased calcium permeability to α3β4 receptors also reported in this study. We thus found no difference in the decay time constants of macroscopic currents between β2-single (leaving α3β4 and α3β4α5 receptors) and α5β2-double KO mice (leaving α3β4 receptors, this study), and rather enhanced calcium transients in response to nAChR activation in α5 KO compared to WT mice (Fischer *et al.*, 2005). In line with our observations, α5 was without effect on the decay time constants in HEK cells transfected with either hα3β4 (495 msec) or hα3α5β4 (563 msec, probed with 300 μM ACh, Nelson *et al.*, 2001).

α3β2 receptors investigated in α5β4-double KO mice distinctly differed from α3β4 receptors by a much faster decay of macroscopic currents and by a low efficacy of cytisine. These cardinal properties have consistently been observed when α3β2 receptors were heterologously expressed in *Xenopus* oocytes (e.g. Papke & Heinemann, 1994; Fenster *et al.*, 1997; Gerzanich *et al.*, 1998) or in HEK 293 cells (Wang *et al.*, 1998). However, data on the potency of agonists when tested on recombinant α3β2 receptors are less consistent by showing e.g. an exceptional low potency of nicotine (Covernton *et al.*, 1994) and a rather high potency of ACh (Luetje & Patrick, 1991). Our own results agree best with the observations in *Xenopus* oocytes by Gerzanich et al. (1998).

Types of nAChRs in the SCG of WT mice

The pharmacological profiles of nAChRs in our single- and double KO models also help in resolving the functions of different nAChRs in the SCG of WT mice. Since cytisine was consistently more potent than DMPP in each and every nerve cell of WT mice (Fischer *et al.*, 2005) we conclude that the α5 subunit is present in all neurons (absence of α5 reversed the cytisine/DMPP potency ratio, see Fischer et al., 2005). The subtle influence of β2 on the effects of agonists (Colquhoun & Patrick, 1997a; Wang *et al.*, 2005) makes it more difficult to establish its impact on α3β4 nAChRs, and although we can not exclude that α3β4β2 receptors are expressed just in a subset of neurons, our observations in β4 KO mice argue against a restricted expression of α3β4β2 nAChRs. In such a case we might expect neurons with α3β2 receptors as well as unresponsive cells without nAChRs (β4 deleted, β2 not present firsthand), a phenomenon we did not observe. We furthermore did not encounter SCG neurons in WT mice with currents that were particular sensitive to α-conotoxin MII and thus propose that all 3 types of receptors occur in all SCG neurons. In keeping with this conclusion, all neurons of the rat SCG showed immunoperoxidase staining with rabbit anti-α5 antibodies (Skok *et al.*, 1999).

Phenotype of mice with deletion of the β4 subunit

Our observation that amplitudes of compound action potentials recorded from postganglionic nerves do not differ between WT and α5β4 KO mice (Fig. 9) indicates that transganglionic neurotransmission is maintained in the SCG of the KO animals. These observations are consistent with a previous report that bradycardia, induced by vagal nerve stimulation at 20 Hz, is not impaired in β4 KO mice (Wang *et al.*, 2003). Although α3β4*

receptors are replaced by α3β2 (Fig. 2C), and although receptors are reduced to < 15 % in the SCG of β4 KO mice (Fig. 1), the number of synaptic nAChRs appears sufficient to trigger action potentials in postsynaptic neurons upon preganglionic nerve activation. A previous observation that smooth muscle contractions of urinary bladder strips and of distal segments of the ileum, induced by bath-applied nAChR agonists, were significantly impaired in the β4 KO (Xu *et al.*, 1999b; Wang *et al.*, 2003) may be explained by the rapid desensitization of ganglionic α3β2 receptors (Fig. 5A, D) that remain in β4 KO mice (Fig. 2D). In contrast to less readily desensitizing α3β4 receptors, α3β2-mediated depolarization of parasympathetic ganglia in response to bath-applied agonists will be short-lasting, with fewer postganglionic nerve action potentials and therefore less transmitter release that cause smooth muscles to contract.

α3 is the only α subunit in the SCG able to form hetero-pentameric nAChRs, and deletion of α3 abolishes synaptic transmission in the SCG of mice (Xu *et al.*, 1999a; Rassadi *et al.*, 2005; Krishnaswamy & Cooper, 2009). Nonetheless, mice lacking α3 are vital and breed even in the absence of functional ganglionic nAChRs (Krishnaswamy & Cooper, 2009). What is important to note is these experiments done in laboratory conditions do not take into account the pressure of survival outside. In humans, both hyper- and under-activity of the autonomic nervous system may cause serious diseases (Xu *et al.*, 1999a; De Biasi, 2002; Lindstrom, 2002; Alkadhi *et al.*, 2005b; Wang *et al.*, 2007).

In our work we have addressed key issues on nAChR composition and function in the mouse sympathetic nervous system by a combined approach of immunoprecipitation, electrophysiology, and deletions of distinct nAChR subunit genes. We show that transganglionic neurotransmission is maintained in our β4 mouse KO models despite significantly reduced levels of nAChRs. Our report confirms some, but not all observations previously made on recombinant α3β4 and α3β2 receptors, stressing the necessity of further such studies on receptors in their native environment.

Supplementary Material

Refer to Web version on PubMed Central for supplementary material.

Acknowledgments

Expert technical assistance was provided by Gabriele Koth and Karin Schwarz. Supported by the Austrian Science Fund, Project P19325-B09, and NIH grants MH53631 and GM48677.

Abbreviations

ACh	acetylcholine
ANOVA	analysis of variance
DMPP	1,1-dimethyl-4-phenylpiperazinium iodide
KO	knockout
MLA	methyllycaconitine
nAChR	nicotinic acetylcholine receptor
P18	postnatal day 18
pA	picoampere
pF	picofarad

PBS	phosphate-buffered saline
SCG	superior cervical ganglion
WT	wild type

References

Albuquerque EX, Pereira EFR, Alkondon M, Rogers SW. Mammalian nicotinic acetylcholine receptors: From structure to function. Physiol. Rev. 2009; 89:73–120. [PubMed: 19126755]

Alkadhi KA, Alzoubi KH, Aleisa AM. Plasticity of synaptic transmission in autonomic ganglia. Prog. Neurobiol. 2005a; 75:83–108. [PubMed: 15784301]

Alkadhi KA, Alzoubi KH, Aleisa AM, Tanner FL, Nimer AS. Psychosocial stress-induced hypertension results from in vivo expression of long-term potentiation in rat sympathetic ganglia. Neurobiol. Dis. 2005b; 20:849–857. [PubMed: 16005635]

Brejc K, van Dijk WJ, Schuurmans M, van der Oost J, Smit AG, Sixma TK. Crystal structure of an ACh-binding protein reveals the ligand-binding domain of nicotinic receptors. Nature. 2001; 411:269–276. [PubMed: 11357122]

Cartier GE, Yoshikami D, Gray WR, Luo S, Olivera BM, McIntosh JM. A new α-conotoxin which targets α3β2 nicotinic acetylcholine receptors. J. Biol. Chem. 1996; 271:7522–7528. [PubMed: 8631783]

Champtiaux N, Changeux J-P. Knockout and knockin mice to investigate the role of nicotinic receptors in the central nervous system. Progr. Brain Res. 2004; 145:235–251.

Champtiaux N, Gotti C, Cordero-Erausquin M, David DJ, Przybylski C, Lena C, Clementi F, Moretti M, Rossi FM, Le Novere N, McIntosh JM, Gardier AM, Changeux J-P. Subunit composition of functional nicotinic receptors in dopaminergic neurons investigated with knock-out mice. J. Neurosci. 2003; 23:7820–7829. [PubMed: 12944511]

Chavez-Noriega LE, Crona JH, Washburn MS, Urrutia A, Elliott KJ, Johnson EC. Pharmacological characterization of recombinant human neuronal nicotinic acetylcholine receptors hα2β2, hα2β4, hα3β2, hα3β4, hα4β2, hα4β4, and hα7 expressed in *Xenopus* oocytes. J. Pharmacol. Exp. Ther. 1997; 280:346–356. [PubMed: 8996215]

Colquhoun LM, Patrick J. α3, β2, and β4 form heterotrimeric neuronal nicotinic acetylcholine receptors in *Xenopus* oocytes. J. Neurochem. 1997a; 69:2355–2362. [PubMed: 9375666]

Colquhoun LM, Patrick JW. Pharmacology of neuronal nicotinic acetylcholine receptor subtypes. Adv. Pharmacol. 1997b; 39:191–220. [PubMed: 9160116]

Corringer P-J, Le Novere N, Changeux J-P. Nicotinic receptors at the amino acid level. Ann. Rev. Pharmacol. Toxicol. 2000; 40:431–458. [PubMed: 10836143]

Covernton PJO, Kojima H, Sivilotti LG, Gibb AJ, Colquhoun D. Comparison of neuronal nicotinic receptors in rat sympathetic neurones with subunit pairs expressed in *Xenopus* oocytes. J. Physiol. 1994; 481:27–34. [PubMed: 7853248]

Cuevas J, Roth AL, Berg DK. Two distinct classes of functional α7-containing nicotinic receptor on rat superior cervical ganglion neurons. J. Physiol. 2000; 525:735–746. [PubMed: 10856125]

De Biasi M. Nicotinic mechanisms in the autonomic control of organ systems. J. Neurobiol. 2002; 53:568–589. [PubMed: 12436421]

De Koninck P, Cooper E. Differential regulation of neuronal nicotinic ACh receptor subunit genes in cultured neonatal rat by sympathetic neurons: Specific induction of α7 by membrane depolarization of a Ca2+/calmodulin dependent pathway. J. Neurosci. 1995; 15:7966–7978. [PubMed: 8613734]

Del Signore A, Gotti C, De Stefano ME, Moretti M, Paggi P. Dystrophin stabilizes α3- but not α7-containing nicotinic acetylcholine receptor subtypes at the postsynaptic apparatus in the mouse superior cervical ganglion. Neurobiol. Dis. 2002; 10:54–66. [PubMed: 12079404]

Fenster CP, Rains MF, Noerager B, Quick MW, Lester RAJ. Influence of subunit composition on desensitization of neuronal acetylcholine receptors at low concentrations of nicotine. J. Neurosci. 1997; 17:5747–5759. [PubMed: 9221773]

Europe PMC Funders Author Manuscripts

Fischer H, Orr-Urtreger A, Role LW, Huck S. Selective deletion of the α5 subunit differentially affects somatic-dendritic versus axonally targeted nicotinic ACh receptors in mouse. J. Physiol. 2005; 563:119–137. [PubMed: 15611037]

Gerzanich V, Wang F, Kuryatov A, Lindstrom J. α5 Subunit alters desensitization, pharmacology, Ca^{+} $^{+}$ permeability and Ca^{++} modulation of human neuronal α3 nicotinic receptors. J. Pharmacol. Exp. Ther. 1998; 286:311–320. [PubMed: 9655874]

Gotti C, Zoli M, Clementi F. Brain nicotinic acetylcholine receptors: native subtypes and their relevance. Trends Pharmacol. Sci. 2006; 27:482–491. [PubMed: 16876883]

Houghtling RA, Davila-Garcia MI, Kellar KJ. Characterization of (+/−)-(3H)epibatidine binding to nicotinic cholinergic receptors in rat and human brain. Mol. Pharmacol. 1995; 48:280–287. [PubMed: 7651361]

Hurst RS, Hajos M, Raggenbass M, Wall TM, Higdon NR, Lawson JA, Rutherford-Root KL, Berkenpas MB, Hoffmann WE, Piotrowski DW, Groppi VE, Allaman G, Ogier R, Bertrand S, Bertrand D, Arneric SP. A novel positive allosteric modulator of the α7 neuronal nicotinic acetylcholine receptor: In vitro and in vivo characterization. J. Neurosci. 2005; 25:4396–4405. [PubMed: 15858066]

Kedmi M, Beaudet AL, Orr-Urtreger A. Mice lacking neuronal acetylcholine receptor β4- subunit and mice lacking both α5- and β4-subunits are highly resistant to nicotine-induced seizures. Physiol. Genomics. 2004; 17:221–229. [PubMed: 14996991]

Krishnaswamy A, Cooper E. An activity-dependent retrograde signal induces the expression of the high-affinity choline transporter in cholinergic neurons. Neuron. 2009; 61:272–286. [PubMed: 19186169]

Kristufek D, Stocker E, Boehm S, Huck S. Somatic and prejunctional nicotinic receptors in cultured rat sympathetic neurones show different agonist profiles. J. Physiol. 1999; 516:739–756. [PubMed: 10200422]

Lewis TM, Harkness PC, Sivilotti LG, Colquhoun D, Millar NS. The ion channel properties of rat recombinant neuronal nicotinic receptor are dependent on the host cell type. J. Physiol. 1997; 505:299–306. [PubMed: 9423173]

Lindstrom J. Autoimmune diseases involving nicotinic receptors. J. Neurobiol. 2002; 53:656–665. [PubMed: 12436428]

Luetje CW, Patrick J. Both α- and β-subunits contribute to the agonist sensitivity of neuronal nicotinic acetylcholine receptors. J. Neurosci. 1991; 11:837–845. [PubMed: 1705971]

Luo S, Kulak JM, Cartier GE, Jacobsen RB, Yoshikami D, Olivera BM, McIntosh JM. α-Conotoxin AuIB selectively blocks α3β4 nicotinic acetylcholine receptors and nicotine-evoked norepinephrine release. J. Neurosci. 1998; 18:8571–8579. [PubMed: 9786965]

Mandelzys A, De Koninck P, Cooper E. Agonist and toxin sensitivities of ACh-evoked currents on neurons expressing multiple nicotinic receptor subunits. J. Neurophysiol. 1995; 74:1212–1221. [PubMed: 7500145]

Mao D, Yasuda RP, Fan H, Wolfe BB, Kellar KJ. Heterogeneity of nicotinic cholinergic receptors in rat superior cervical and nodosa ganglia. Mol. Pharmacol. 2006; 70:1693–1699. [PubMed: 16882879]

McGehee DS, Role LW. Physiological diversity of nicotinic acetylcholine receptors expressed by vertebrate neurons. Annu. Rev. Physiol. 1995; 57:521–546. [PubMed: 7778876]

Millar NS. RIC-3: A nicotinic acetylcholine receptor chaperone. Br. J. Pharmacol. 2008; 153:S177–S183. [PubMed: 18246096]

Moser N, Mechawar N, Jones I, Gochberg-Sarver A, Orr-Urtreger A, Plomann M, Salas R, Molles B, Marubio L, Roth U, Maskos U, Winzer-Serhan U, Bourgeois JP, Le Sourd AM, De Biasi M, Schroder H, Lindstrom J, Maelicke A, Changeux JP, Wevers A. Evaluating the suitability of nicotinic acetylcholine receptor antibodies for standard immunodetection procedures. J. Neurochem. 2007; 102:479–492. [PubMed: 17419810]

Nai Q, McIntosh JM, Margiotta JF. Relating neuronal nicotinic acetylcholine receptor subtypes defined by subunit composition and channel function. Mol Pharmacol. 2003; 63:311–324. [PubMed: 12527802]

Nelson ME, Kuryatov A, Choi CH, Zhou Y, Lindstrom J. Alternate stoichiometries of α4β2 nicotinic acetylcholine receptors. Mol. Pharmacol. 2003; 63:332–341. [PubMed: 12527804]

Nelson ME, Wang F, Kuryatov A, Choi CH, Gerzanich V, Lindstrom J. Functional properties of human nicotinic AChRs expressed by IMR-32 neuroblastoma cells resemble those of α3β4 AChRs expressed in permanently transfected HEK cells. J. Gen. Physiol. 2001; 118:563–582. [PubMed: 11696612]

Orr-Urtreger A, Göldner FM, Saeki M, Lorenzo I, Goldberg L, De Biasi M, Dani JA, Patrick JW, Beaudet AL. Mice deficient in the α7 neuronal nicotinic acetylcholine receptor lack α-bungarotoxin binding sites and hippocampal fast nicotinic currents. J. Neurosci. 1997; 17:9165–9171. [PubMed: 9364063]

Papke RL, Bencherif M, Lippiello PM. An evaluation of neuronal nicotinic acetylcholine receptor activation by quaternary nitrogen compounds indicates that choline is selective for the α7 subtype. Neurosci. Lett. 1996; 213:201–204. [PubMed: 8873149]

Papke RL, Heinemann SF. Partial agonist properties of cytisine on neuronal nicotinic receptors containing the β2 subunit. Mol. Pharmacol. 1994; 45:142–149. [PubMed: 8302273]

Picciotto MR, Zoli M, Lena C, Bessis A, Lallemand Y, Le Novere N, Vincent P, Pich EM, Brulet P, Changeux J-P. Abnormal avoidance learning in mice lacking functional high-affinity nicotine receptor in the brain. Nature. 1995; 374:65–67. [PubMed: 7870173]

Pollock VV, Pastoor T, Katnik C, Cuevas J, Wecker L. Cyclic AMP-dependent protein kinase A and protein kinase C phosphorylate α4β2 nicotinic receptor subunits at distinct stages of receptor formation and maturation. Neuroscience. 2009; 158:1311–1325. [PubMed: 19101612]

Putz G, Kristufek D, Orr-Urtreger A, Changeux JP, Huck S, Scholze P. Nicotinic acetylcholine receptor-subunit mRNAs in the mouse superior cervical ganglion are regulated by development but not by deletion of distinct subunit genes. J. Neurosci. Res. 2008; 86:972–981. [PubMed: 17975828]

Rae J, Cooper K, Gates P, Watsky M. Low access resistance perforated patch recordings using amphotericin B. J. Neurosci. Meth. 1991; 37:15–26.

Rassadi S, Krishnaswamy A, Pie B, McConnell R, Jacob MH, Cooper E. A null mutation for the α3 nicotinic acetylcholine (ACh) receptor gene abolishes fast synaptic activity and reveals that ACh output from developing preganglionic terminals is regulated in an activity-dependent manner. J. Neurosci. 2005; 25:8555–8566. [PubMed: 16162937]

Scholze P, Orr-Urtreger A, Changeux JP, McIntosh JM, Huck S. Catecholamine outflow from mouse and rat brain slice preparations evoked by nicotinic acetylcholine receptor activation and electrical field stimulation. Br. J. Pharmacol. 2007; 151:414–422. [PubMed: 17401441]

Severance EG, Zhang H, Cruz Y, Pakhlevaniants S, Hadley SH, Amin J, Wecker L, Reed C, Cuevas J. The α7 nicotinic acetylcholine receptor subunit exists in two isoforms that contribute to functional ligand-gated ion channels. Mol Pharmacol. 2004; 66:420–429. [PubMed: 15322233]

Sharples CGV, Kaiser S, Soliakov L, Marks MJ, Collins AC, Washburn M, Wright E, Spencer JA, Gallagher T, Whiteaker P, Wonnacott S. UB-165: A novel nicotinic agonist with subtype selectivity implicates the α4β2* subtype in the modulation of dopamine release from rat striatal synaptosomes. J. Neurosci. 2000; 20:2783–2791. [PubMed: 10751429]

Sivilotti LG, McNeil DK, Lewis TM, Nassar MA, Schoepfer R, Colquhoun D. Recombinant nicotinic receptors, expressed in *Xenopus* oocytes, do not resemble native rat sympathetic ganglion receptors in single-channel behaviour. J. Physiol. 1997; 500:123–138. [PubMed: 9097938]

Skok MV, Voitenko LP, Voitenko SV, Lykhmus EY, Kalashnik EN, Litvin TI, Tzartos SJ, Skok VI. Alpha subunit composition of nicotinic acetylcholine receptors in the rat autonomic ganglia neurons as determined with subunit-specific anti-α(181-192) peptide antibodies. Neuroscience. 1999; 93:1427–1436. [PubMed: 10501468]

Wang F, Gerzanich V, Wells GB, Anand R, Peng X, Keyser K, Lindstrom J. Assembly of human neuronal nicotinic receptor α5 Subunits with α3, β2, and β4 subunits. J. Biol. Chem. 1996; 271:17656–17665. [PubMed: 8663494]

Wang F, Nelson ME, Kuryatov A, Olale F, Cooper J, Keyser K, Lindstrom J. Chronic nicotine treatment up-regulates human α3β2 but not α3β4 acetylcholine receptors stably transfected in human embryonic kidney cells. J. Biol. Chem. 1998; 273:28721–28732. [PubMed: 9786868]

Wang N, Orr-Urtreger A, Chapman J, Ergun Y, Rabinowitz R, Korczyn AD. Hidden function of neuronal nicotinic acetylcholine receptor β2 subunits in ganglionic transmission: comparison to α5 and β4 subunits. J. Neurol. Sci. 2005; 228:167–177. [PubMed: 15694199]

Wang N, Orr-Urtreger A, Chapman J, Rabinowitz R, Korczyn AD. Deficiency of nicotinic acetylcholine receptor β4 subunit causes autonomic cardiac and intestinal dysfunction. Mol Pharmacol. 2003; 63:574–580. [PubMed: 12606764]

Wang N, Orr-Urtreger A, Chapman J, Rabinowitz R, Nachmann R, Korczyn AD. Autonomic function in mice lacking α5 neuronal nicotinic acetylcholine receptor subunit. J. Physiol. 2002a; 542:347–354. [PubMed: 12122136]

Wang N, Orr-Urtreger A, Korczyn AD. The role of neuronal nicotinic acetylcholine receptor subunits in autonomic ganglia: lessons from knockout mice. Prog. Neurobiol. 2002b; 68:341–360. [PubMed: 12531234]

Wang Z, Low PA, Jordan J, Freeman R, Gibbons CH, Schroeder C, Sandroni P, Vernino S. Autoimmune autonomic ganglionopathy - IgG effects on ganglionic acetylcholine receptor current. Neurology. 2007; 68:1917–1921. [PubMed: 17536048]

Wong ET, Holstad SG, Mennerick SJ, Hong SE, Zorumski CF, Isenberg KE. Pharmacological and physiological properties of a putative ganglionic nicotinic receptor, α3β4, expressed in transfected eucaryotic cells. Mol. Brain Res. 1995; 28:101–109. [PubMed: 7707862]

Xu W, Gelber S, Orr-Urtreger A, Armstrong D, Lewis RA, Ou CN, Patrick J, Role L, De Biasi M, Beaudet AL. Megacystis, mydriasis, and ion channel defect in mice lacking the α3 neuronal nicotinic acetylcholine receptor. Proc. Natl. Acad. Sci. 1999a; 96:5746–5751. [PubMed: 10318955]

Xu W, Orr-Urtreger A, Nigro F, Gelber S, Sutcliffe CB, Armstrong D, Patrick JW, Role LW, Beaudet AL, De Biasi M. Multiorgan autonomic dysfunction in mice lacking the β2 and the β4 subunits of neuronal nicotinic acetylcholine receptors. J. Neurosci. 1999b; 19:9298–9305. [PubMed: 10531434]

Zhang Z, Vijayaraghavan S, Berg DK. Neuronal acetylcholine receptors that bind α-bungarotoxin with high affinity function as ligand-gated ion channels. Neuron. 1994; 12:167–177. [PubMed: 7507338]

Zoli M, Lena C, Picciotto MR, Changeux J-P. Identification of four classes of brain nicotinic receptors using β2 mutant mice. J. Neurosci. 1998; 18:4461–4472. [PubMed: 9614223]

Zwart R, Vijverberg HPM. Four pharmacologically distinct subtypes of α4β2 nicotinic acetylcholine receptor expressed in *Xenopus laevis* oocytes. Mol. Pharmacol. 1998; 54:1124–1131. [PubMed: 9855643]

Europe PMC Funders Author Manuscripts

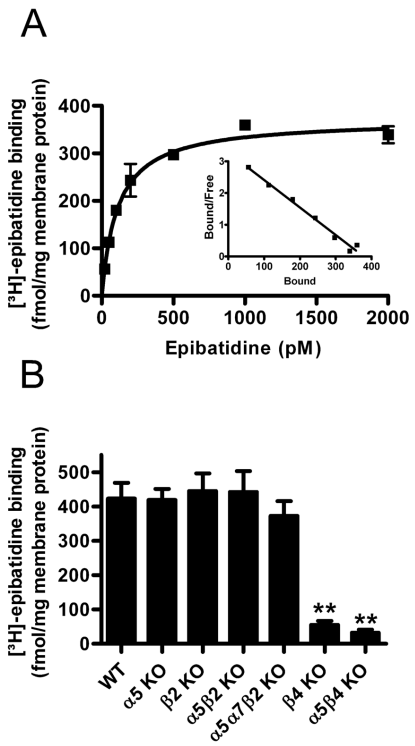

Figure 1. [^{3}H]-epibatidine binding sites are significantly reduced in α5β4-double and β4-single KO mice

A. Kinetics of [^{3}H]-epibatidine binding to membrane homogenates from wild type mouse SCG. Data points are means of specific binding ± SEM of duplicate measurements. Nonspecific binding determined by the presence of 300 μM nicotine was subtracted from overall to obtain specific binding. Parameters of the curve fitted to the data points were 112.6 ± 9.1 pM (KD) and 371.2 ± 13.5 fmol/mg protein (Bmax). Inset: Scatchard plot of data (abscissa: bound [^{3}H]-epibatidine (fmol/mg); ordinate: bound/free [^{3}H]-epibatidine (fmol/mg protein)/pM)). Averaged kinetic parameters ± SEM from 4 such experiments were 150.7 ± 25.6 pM (KD) and 345.8 ± 25.6 fmol/mg protein (Bmax).

B. Specific binding of 1 nM [^{3}H]-epibatidine to SCG membrane homogenates taken from wild type mice and from mice with distinct deletions of indicated nAChR subunit genes. Data are means ± SEM of 3-10 independent experiments, each performed with triplicate measurements. Compared to WT SCG, [^{3}H]-epibatidine binding was significantly reduced only in α5β4-double and β4-single KO animals (one-way ANOVA, $F = 35{,}46$, $P < 0.0001$, followed by Dunnett's *post-hoc* test, $^{**}P < 0.01$). [^{3}H]-epibatidine binding sites did not differ significantly between α5β4-double (7.8 % of WT) and β4-single KO animals (13.2 % of WT, Student's *t*-test).

Europe PMC Funders Author Manuscripts

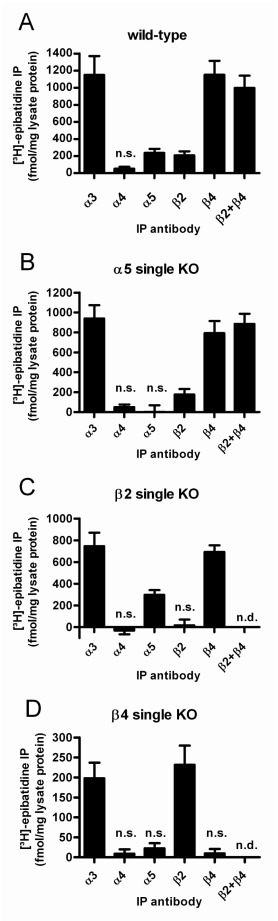

Figure 2. Subunit composition of nAChRs in the wild-type mouse SCG, and absence of compensation in the SCG of mice with deletions of a single nAChR subunit gene

nAChRs from SCG membranes of wild-type mice (Panel A) or mice with deletions of the α5 (Panel B), the β2 (Panel C), or the β4 subunits (Panel D) were solubilized, labeled with 1 nM [^{3}H]-epibatidine and immunoprecipitated with each of the subunit-specific antibodies indicated at the abscissa. Nonspecific binding was measured in the presence of 300 μM nicotine and subtracted from overall to obtain the specific binding shown in the figure. Data are means ± SEM of 4-8 independent experiments, each performed with triplicate (panels A, B and C) or duplicate (panel D) measurements. Note in Panels A and B that anti-α3 and anti-β4 antibodies precipitate an identical number of receptors, and that the combined use of anti-β4 and anti-β2 antibodies does not precipitate more receptors than the single use of anti-β4 antibodies. The levels of α4 are not significantly different from zero ($P = 0.052$ in Panel A and $P = 0.189$ in Panel B, one sample Students *t*-test). Anti-α5 and anti-β2 antibodies precipitated 24 % and 21 %, respectively, of the receptors that were precipitated by the combined use of anti-β4 and anti-β2 measurements. n.s: not significantly different from zero ($P > 0.05$, one sample Students *t*-test). n.d.: not determined.

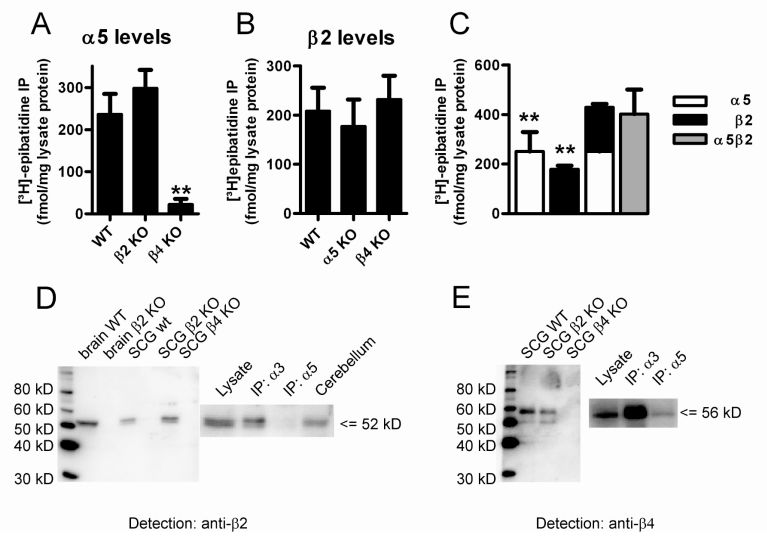

Figure 3. Subunit composition of nAChRs in the mouse SCG

A. The α5 subunit co-assembles with β4 only and is not up-regulated in the SCG of β2 KO mice. nAChRs from SCG membranes of WT, β2, and β4 KO mice (indicated at the abscissa) were solubilized, labeled with 1 nM [^{3}H]-epibatidine, and immunoprecipitated with our anti-α5 antibody. Data are the mean specific binding ± SEM of 3-8 independent experiments, each performed with triplicate measurements. Note that levels of the α5 subunit do not significantly differ between WT and β2 KO animals. In contrast, α5 is lost in the SCG of β4 KO mice (not significantly different from zero, $P > 0.05$, one sample Students *t*-test). All columns were compared using one-way ANOVA, $F = 10.38$, $P = 0.0008$, followed by a Dunnett's *post-hoc* multiple comparison test: WT *vs* β2 KO: $P > 0.05$; WT *vs* β4 KO: $P < 0.01$)

B. The β2 subunit does not compensate for the absence of either α5 or β4. nAChRs solubilized and labeled as described above were immunoprecipitated with our anti-β2 antibody. Data are the mean specific binding ± SEM of 4-6 independent experiments, each performed with triplicate measurements. Note that β2 levels do not differ significantly between the 3 genotypes indicated at the abscissa (one-way ANOVA, $F = 0.227$, $P = 0.800$).

C. The subunits α5 and β2 do not co-assemble in the same receptor. nAChRs solubilized and labeled as described above were immunoprecipitated in parallel with anti-α5 (white bars), anti-β2 (black bars), or a combination of both antibodies (grey bar). Data are the mean specific binding ± SEM of 5 independent experiments, each performed with triplicate measurements. The number of receptors immunoprecipitated by each of the single antibodies differed significantly from the number of receptors precipitated by a combination of the two antibodies ($P < 0.01$). The arithmetic sum of the two individual precipitations is not significantly different from the result obtained by combined immunoprecipitation with both antibodies (repeated measures one-way ANOVA $F = 14.72$, $P = 0.0003$, followed by a Dunnett's multiple comparison test with data referenced to the result obtained by the combined immunoprecipitation with both antibodies).

D. The α5 subunit does not co-assemble with β2. The left part of the figure illustrates the specificity of our anti-β2 antibody for Western blot analyses. Note bands of approximately 52 kD in brain and SCG samples from WT and β4 KO animals, and the absence of such bands in β2 KO mice. As shown on the right part of the figure, the band can also be detected in Western blots of receptors immunoprecipitated with anti-α3, but not with anti-α5 antibodies. The cerebellum is added as a further positive control.

E. The α5 subunit co-assembles with β4. The left part of the figure shows the specificity of our anti-β4 antibody for Western blot analyses. Note major band of approximately 56 kD

Europe PMC Funders Author Manuscripts

in SCG samples from WT and β2 KO mice and the absence of such a band in β4 KO animals. The anti-β4 antibody detects a solid band in Western blots of receptors immunoprecipitated with anti-α3, and a much weaker band if receptors were immunoprecipitated with anti-α5 antibodies (right part of the figure).

Europe PMC Funders Author Manuscripts

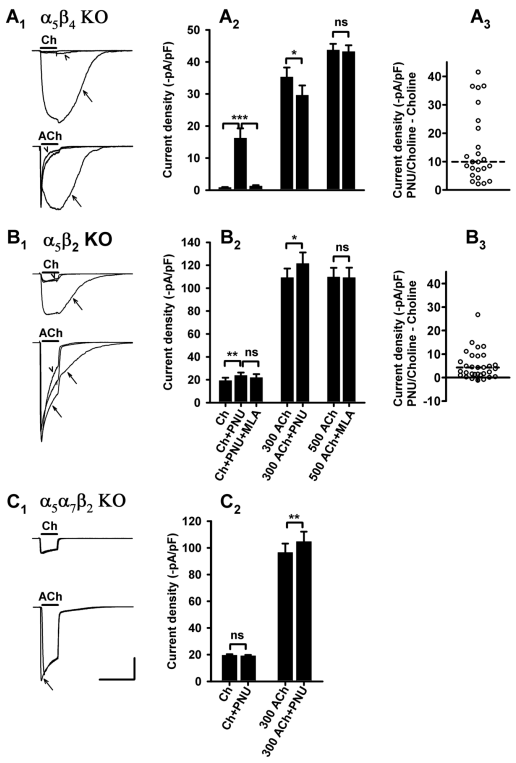

Figure 4. Probing α7 nAChRs

A. Patch clamp measurements of SCG neurons from α5β4 KO animals. **A1, upper panel**: Unveiling of α7-mediated currents by the type II positive allosteric modulator PNU-120596, and rapid reversal of the effect by methyllycaconitine (MLA). The figure shows a particularly large effect of PNU-120596. 3 superimposed current traces in response to 10 mM choline (Ch, indicated by bar); 10 mM choline in the presence of - and following a 10 sec superfusion with - 10 μM PNU-120596 (arrow); pretreatment with 5 nM MLA for 2 min, followed by 10 mM choline plus 10 μM PNU-120596 (arrowhead). Note that choline by itself has a negligible effect. Calibration: 4 sec, 1 nA. **A1, lower panel**: Same cell, with currents induced by 300 μM ACh (in the presence of 0.1 μM atropine, bar). 10 μM PNU-120596 (arrow) has no effect on initial peak current but gives rise to a large second peak of delayed onset (arrow). Arrowhead denotes current following pretreatment with MLA. Calibration: 4 sec, 1 nA **A2**. See panel B2 for a labeling of bars. Choline-induced currents in the presence of 10 μM PNU-120596 (Ch+PNU) are significantly larger than in the absence of PNU (Ch) or after a 2 min pretreatment with 5 nM MLA (Ch+PNU+MLA). Paired observations of 18 neurons ($P = 0.0002$, Wilcoxon test). Peak currents in response to 300 μM ACh are somewhat reduced ($P = 0.0315$, paired Student's *t*-test, n = 13 neurons) in the presence of 10 μM PNU-120596 (300 ACh+PNU). Peak currents in response to 500 μM ACh are unaffected by a 2 min pretreatment with 5 nM MLA (500 ACh+MLA) (n = 22 neurons, $P = 0.6041$, paired Student's *t*-test). **A3**. Net effect of 10 μM PNU-120596 obtained by subtracting the peak current in response to 10 mM choline from choline-induced current in the presence of PNU-120596. Dashed line indicates a Median value of 9.90 pA/pF (n = 24 cells).

B. Patch clamp measurements of SCG neurons from α5β2 KO animals. **B1, upper panel**: Unveiling of α7-mediated currents by PNU-120596, and rapid reversal of the effect by MLA. The figure shows a particularly large effect of PNU-120596. 3 superimposed current traces in response to 10 mM choline (Ch, indicated by bar); 10 mM choline in the presence

of - and following a 10 sec superfusion with - 10 μM PNU-120596 (arrow); pretreatment with 5 nM MLA for 2 min, followed by 10 mM choline plus 10 μM PNU-120596 (arrowhead). Note that choline by itself has a noticeable effect by activating α3β4 nAChRs. Calibration: 4 sec, 2 nA. **B1, lower panel**: Same cell, with currents induced by 300 μM ACh (in the presence of 0.1 μM atropine, bar). 10 μM PNU-120596 (arrows) has no effect on initial peak current but slows the decay of the current and the washout. Arrowhead denotes current following pretreatment with MLA. Calibration: 4 sec, 2 nA. **B2**. Choline-induced currents in the presence of 10 μM PNU-120596 (Ch+PNU) are significantly larger than in the absence of PNU (Ch). Paired observations of 16 neurons ($P = 0.0015$, Wilcoxon test). The inhibition of currents in response to choline plus PNU-120596 (Ch+PNU) by a 2 min pretreatment with 5 nM MLA (Ch+PNU+MLA) is statistically not significant ($P = 0.4156$, Wilcoxon test, n = 16). Peak currents in response to 300 μM ACh are somewhat enhanced in the presence of 10 μM PNU-120596 (300 ACh+PNU). N = 14 neurons ($P = 0.0163$, paired Student's *t*-test). Peak currents in response to 500 μM ACh are unaffected by a 2 min pretreatment with 5 nM MLA (500 ACh+MLA). N = 25 neurons ($P = 0.9692$, paired Student's *t*-test). **B3**. Net effect of 10 μM PNU-120596 obtained by subtracting the peak current in response to 10 mM choline from choline-induced current in the presence of PNU-120596. Dashed line indicates a Median value of 4.29 pA/pF (n = 33 cells). These data differ significantly from the data shown in panel A3 ($P = 0.0023$, Mann-Whitney test). **C.** Patch clamp measurements of SCG neurons from α5α7β2 KO animals. **C1, upper panel**: Currents in response to 10 mM choline (bar) are unaffected by 10 μM PNU-120596. Graph shows two superimposed current traces. The schedule of substance application is identical to panels A1 and B1. Calibration: 4 sec, 2 nA. **C1, lower panel**: Same cell, with currents induced by 300 μM ACh (in the presence of 0.1 μM atropine, bar). 10 μM PNU-120596 (arrow) has no effect on the time course of receptor desensitization and the washout of ACh. Calibration: 4 sec, 2 nA. **C2**. Choline-induced currents in the presence of 10 μM PNU-120596 (Ch+PNU) are not significantly different from currents in the absence of PNU (Ch). Paired observations of 35 neurons ($P = 0.1918$, Wilcoxon test). Peak currents in response to 300 μM ACh are somewhat enhanced in the presence of 10 μM PNU-120596 (300 ACh+PNU). N = 26 neurons ($P = 0.0026$, paired Student's *t*-test).

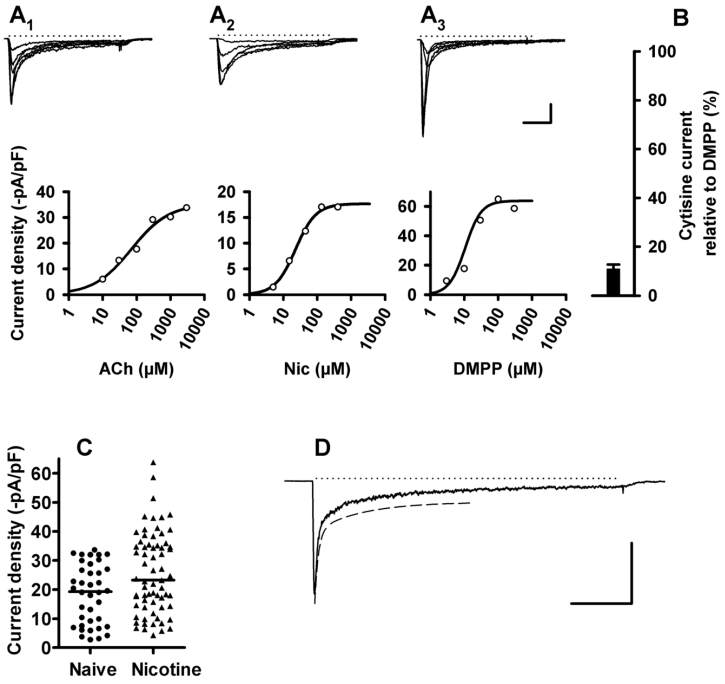

Figure 5. Functional properties of α3β2 nAChRs (analyzed in α5β4 KO mice)

A1-3. Agonist-induced currents (upper panels; applications indicated by dotted lines), and corresponding concentration-response curves (lower panels) by the nAChR agonists ACh (A1, in the presence of 0.1 μM atropine), nicotine (A2), and 1,1-dimethyl-4-phenylpiperazinium iodide (DMPP) (A3). In order to construct the dose-response curves, peak current amplitudes were fitted to the logistic equation shown in Methods. Averaged fit parameters are provided in Table 1. Calibration A1-A3: 500 msec; 0.5 nA.

B. Low efficacy of cytisine at α3β2 receptors: Maxima taken from full DMPP dose response curves were set in relation to responses by saturating concentrations of cytisine in the same cell. Cytisine at saturating concentrations produced only 10.76 ± 1.59 % of the effect of DMPP (n = 8).

C. α3β2 nAChR up-regulation by nicotine: Peak currents in response to 300 μM ACh (in the presence of 0.1 μM atropine) in untreated cultures (Naïve; circles; n = 38), and in cultures treated for > 48 h with 100 μM nicotine (Nicotine; triangles; n = 67). Lines indicate the Median values 19.3 and 23.2 pA/pF, for naïve and nicotine-treated cultures, respectively; significantly different at $P = 0.0087$, Mann-Whitney test.

D: Rapid desensitization of α3β2 nAChR. Patch clamp recording of a SCG neuron taken from a α5β4 KO mouse, with current induced by 300 μM ACh (in the presence of 0.1 μM atropine, dotted line). Dashed line indicates decay of current fitted to the sum of two exponential functions (displaced for clarity from original trace by 200 pA). Fit parameters are 115 msec (T_f, fast), 1477 msec (T_s, slow), −1171 pA (A_f, fast), −472 pA (A_s, slow), −140 pA (plateau). Calibration: 2 sec, 1 nA. Averaged fit parameters from identically designed experiments are provided in Table 2.

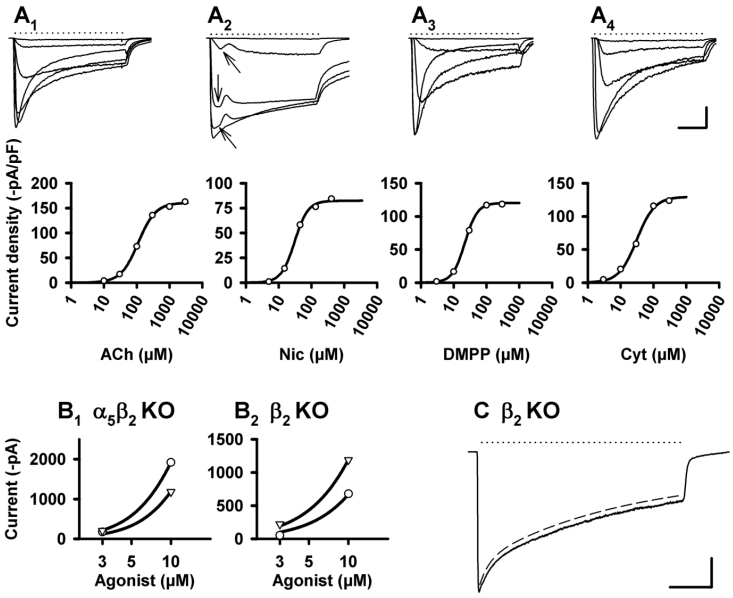

Figure 6. Functional properties of α3β4 nAChRs (in α5β2 KO mice)

A. Agonist-induced currents (upper panels; applications indicated by dotted lines), and corresponding concentration-response curves (lower panels) by the nAChR agonists ACh (A1, in the presence of 0.1 μM atropine), nicotine (A2), DMPP (A3), and cytisine (A4). Arrows in A2 indicate an initial "hump" discussed in the Results section. In order to construct the dose-response curves, peak current amplitudes were fitted to the logistic equation shown in Methods. Averaged fit parameters are provided in Table 1. Calibration A1-A4: 500 msec; 2 nA.

B. Potency ratios determined from agonist-induced peak currents elicited at the low end of the concentration-response curves. **B1. α5β2 KO**: Peak current amplitudes in response to 3 and 10 μM DMPP (circles) and cytisine (triangles), respectively, were fitted to the logistic equation with the constraints of a common slope and a maximum set to 7 nA. This resulted in fictitious EC_{50} values of 16.1 μM (DMPP) and 21.7 μM (cytisine) and a potency ration of 21.7/16.1 = 1.34. **B2. β2 KO**: Same protocol as described for panel B1. Fictitious EC_{50} values were 39.2 μM (DMPP) and 26.2 μM (cytisine), with a resulting potency ration of 0.67. Note that cytisine is more potent than DMPP in the β2 KO, whereas potencies are reversed in the α5β2 double KO. Averaged potency ratios from identically designed experiments are provided in Fig. 7.

C. Patch clamp recording of a SCG neuron taken from a β2 KO mouse, with current induced by 300 μM ACh in the presence of 0.1 μM atropine (dotted line). Dashed line indicates decay of current fitted to the sum of two exponential functions (displaced for clarity from original trace by 200 pA). Fit parameters are 0.47 sec (T_f, fast), 6.98 sec (T_s, slow), −809 pA (A_f, fast), −2899 pA (A_s, slow), −943 pA (plateau). Calibration: 2 sec, 1 nA. Averaged fit parameters from identically designed experiments are provided in Table 2.

Europe PMC Funders Author Manuscripts

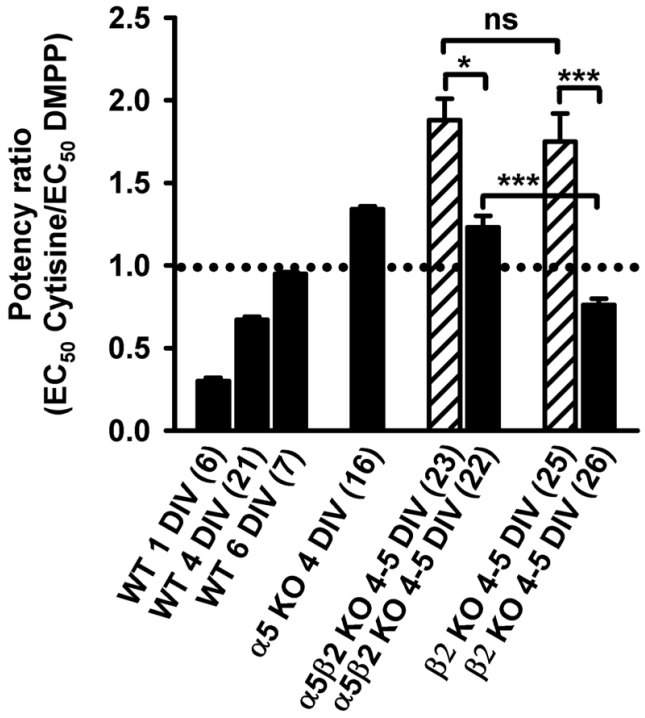

Figure 7. Genotypes differ by their cytisine to DMPP potency ratios

Filled bars show mean ± SEM low-concentration potency ratios; hatch bars are mean ± SEM potency ratios deduced from full concentration-response curves of genotypes indicated at the abscissa. Potency ratios of cytisine by DMPP were calculated for individual cells by dividing the corresponding fictitious EC_{50} values (low concentration, see Fig. 6B for an example) or fully explored EC_{50} values (full concentration-response). Figures in parenthesis are the number of cells. The data for WT and α5 KO are from Fischer et al. (2005). Ratios > 1 (above the dotted line) indicate a higher potency of DMPP. One-way ANOVA ($F = 28.47$, $P < 0.0001$), followed by Newman-Keuls multiple comparison test. n.s. not significantly different ($P > 0.05$); * significantly different ($P < 0.05$); *** significantly different ($P < 0.001$).

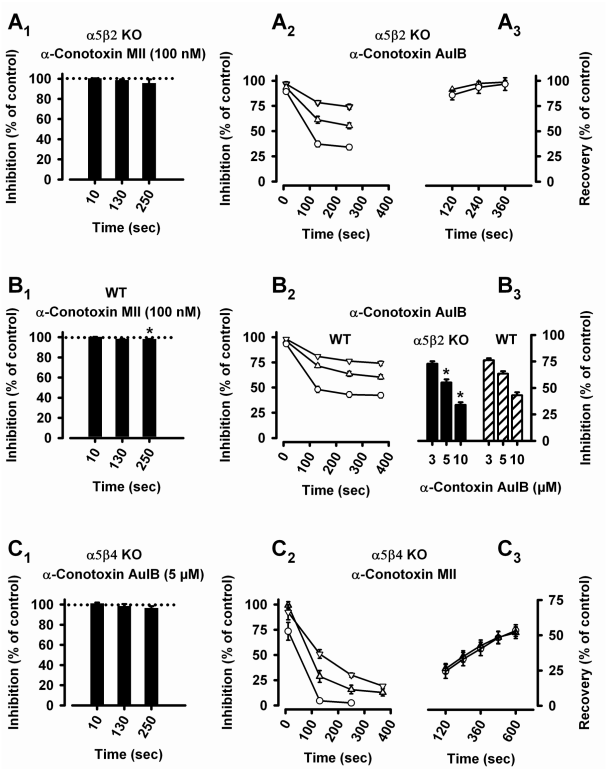

Figure 8. Effects of the α-conotoxins AuIB and MII

Currents were induced by 300 μM ACh (in the presence of 0.1 μM atropine, 0.5 μM TTX, and 0.1 mg/ml bovine serum albumin) in cultured SCG neurons of α5β2 KO (A1-A3, B3), WT (B1-B3), or α5β4 KO (C1-C3) mice, and in the absence (control, 100 %) or presence of the α-conotoxins AuIB or MII.

A1. α5β2 KO mice: Bars (mean percentage of currents relative to controls ± SEM, n = 7-9 cells) show the absence of effects of α-conotoxin MII on nAChRs in SCG neurons of α5β2 KO mice. The application of 100 nM α-conotoxin MII for indicated periods of time does not significantly decrease peak currents (one sample Student's *t*-test with reference to a hypothetical 100 %: $P_{10\ sec} = 0.6752$; $P_{130\ sec} = 0.2009$; $P_{250\ sec} = 0.3046$). **A2.** Time- and concentration-dependent inhibition by α-conotoxin AuIB of nAChRs remaining in SCG neurons of α5β2 KO mice. Triangles down: 3 μM (n = 5 cells); triangles up: 5 μM (n = 8 cells); circles: 10 μM α-conotoxin AuIB (n = 7 cells). Data points are the mean percentages of currents relative to controls ± SEM (shown if error bars exceed symbols). **A3.** Fast and full recovery of the inhibition by 5 μM (triangles down, n = 3 cells) and 10 μM α-conotoxin AuIB (circles, n = 4 cells).

B1. WT mice: Bars (mean percentage of currents relative to controls ± SEM, n = 13 cells) show little effect of α-conotoxin MII on nAChRs in SCG neurons of WT mice. The application of 100 nM α- conotoxin MII for indicated periods of time leaves 100.4 % (after 10 sec, $P = 0.6119$), 98.4 % (after 130 sec, $P = 0.0534$), and 98.2 % (after 250 sec, $P = 0.0498$) of control peak currents (one sample Student's *t*-test with reference to a hypothetical 100 %). **B2.** Time- and concentration-dependent inhibition by α-conotoxin AuIB of nAChRs in SCG neurons of WT mice. Triangles down: 3 μM (n = 8-11 cells); triangles up: 5 μM (n = 13-14 cells); circles: 10 μM α-conotoxin AuIB (n = 8 cells). Data points are the mean percentages of currents relative to controls ± SEM (shown if error bars exceed symbols). **B3**. Concentration-dependent inhibition by indicated concentrations of conotoxin AuIB of nAChR currents in SCG neurons of α5β2 KO (filled bars) or WT (hatched bars)

Europe PMC Funders Author Manuscripts

mice. Currents induced by 300 μM ACh were measured 250 sec after toxin application and set in relation to control peak currents. AuIB has a significantly larger effect in α5β2 KO than in WT mice (AuIB at 5 μM: α5β2 KO: 55.2 ± 2.9 %, n = 8 cells; WT: 63 ± 2.4 %, n = 14 cells; $P = 0.0483$, Student's *t*-test; AuIB at 10 μM: α5β2 KO: 34.0 ± 2.5 %, n = 7 cells; WT: 43.0 ± 3.0 %, n = 8 cells; $P = 0.0414$, Student's *t*-test).

C1. α5β4 KO mice: Bars (mean percentage of currents relative to controls ± SEM, n = 8 cells) show the absence of effects of α-conotoxin AuIB on nAChRs in SCG neurons of α5β4 KO mice. The application of 5 μM α-conotoxin AuIB for indicated periods of time does not significantly inhibit peak currents (one sample Student's *t*-test with reference to a hypothetical 100 %: $P_{10\ sec} = 0.1173$; $P_{130\ sec} = 0.5057$; $P_{250\ sec} = 0.0935$). **C2**. Time- and concentration-dependent inhibition by α-conotoxin MII of nAChRs remaining in SCG neurons of α5β4 KO mice. Triangles down: 10 nM (n = 8 cells); triangles up: 30 nM (n = 11 cells); circles: 100 nM α-conotoxin MII (n = 6 cells). Data points are the mean percentages of currents relative to controls ± SEM (shown if error bars exceed symbols). Note that a 130 sec exposure to 100 nM α-conotoxin MII blocks 95 % of the currents. **C3**: Slow and partial recovery of the inhibition by 30 nM (triangles up, n = 9 cells) and 100 nM α-conotoxin MII (circles, n = 6 cells).

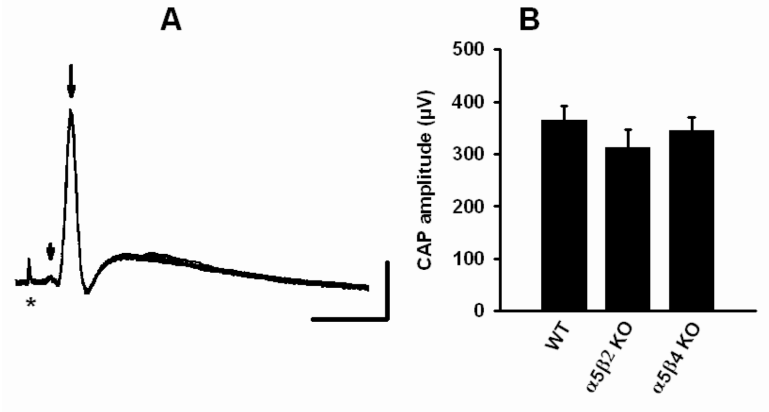

Figure 9. Compound action potentials do not differ between genotypes

A. Postganglionic compound action potentials (20 superimposed traces) recorded from the postganglionic (internal carotid) nerve in response to suprathreshold stimuli at 0.5 Hz to the preganglionic (SCG) nerve. Arrow shows the compound action potential, arrowhead the preganglionic potential, and asterix the stimulation artifact. The ganglion was taken from a 5 weeks old WT animal. Calibration: 20 msec, 200 μV.

B: Bars show mean ± SEM compound action potential amplitudes measured in SCGs taken from 4-6 weeks old WT (n = 20), α5β2 KO (n = 14), and α5β4 KO (n = 16) mice. Note that mean amplitudes of either α5β2 KO or α5β4 do not differ significantly from WT ($P > 0.05$, one-way ANOVA ($F = 0.8223$, $P = 0.4457$), followed by a Dunnett's multiple comparison test with data referenced to WT).

Europe PMC Funders Author Manuscripts

Table 1
Pharmacological properties of distinct nAChRs

The table shows the data of averaged fit parameters from dose-response curves of individual cells (n = number of cells). (A) α3β4 receptors (see Fig. 6 for original current traces). (B) α3β4α5 receptors. SCG neurons of β2 KO mice contain about 60 % α3β4 and 40 % α3β4α5 receptors (see Fig. 2B). (C) α3β2 receptors (see Fig. 5 for original current traces).

A. α3β4 receptors (in the α5β2 KO)	**DMPP (n = 26)**	**Cytisine (n = 24)**	**Nicotine (n = 25)**	**ACh (n = 24)**
EC_{50}	19.04 ± 0.76	34.5 ± 2.26	32.95 ± 1.34	101.4 ± 4.65
Hill coefficient	1.91 ± 0.06	1.44 ± 0.06	1.68 ± 0.06	1.60 ± 0.05
Max current density (−pA/pF)	107.8 ± 6.7[1]	124.5 ± 9.2[1]	115.6 ± 7.9[1]	134.79 ± 11.2[1]

B. α3β4α5 receptors (in the β2 KO)	**DMPP (n = 26)**	**Cytisine (n = 26)**	**n.d.**	**n.d.**
EC_{50}	23.03 ± 1.17	37.69 ± 2.43		
Hill coefficient	1.79 ± 0.08	1.10 ± 0.02		
Max current density (−pA/pF)	91.73 ± 6.30[2]	121.12 ± 8.02[2]		

C. α3β2 receptors (in the α5β4 KO)	**DMPP (n = 8)**	**Cytisine (n = 8)**	**Nicotine (n = 11)**	**ACh (n = 10)**
EC_{50}	10.97 ± 1.79	n.d.	22.51 ± 1.18	168.73 ± 25.20
Hill coefficient	1.21 ± 0.12	n.d.	1.78 ± 0.18	0.67 ± 0.04
Max current density (−pA/pF)	39.29 ± 7.50[3]	10.76 ± 1.59 %[4]	36.20 ± 8.89[3]	34.29 ± 5.81[3]

[1] Not significantly different: One-way ANOVA ($F = 1.742$, $P = 0.1636$), followed by Newman-Keuls multiple comparison test (each comparison with a $P > 0.05$)

[2] Significantly different ($P = 0.0059$, Student's *t*-test)

[3] Not significantly different: One-way ANOVA ($F = 0.09781$, $P = 0.3429$), followed by Newman-Keuls multiple comparison test (each comparison with a $P > 0.05$)

[4] Cytisine at saturating concentrations produced only 10.76 ± 1.59 % of the effect of DMPP at α3β2 receptors (n = 8).

Europe PMC Funders Author Manuscripts

Table 2

The decay of macroscopic currents differs significantly between α3β4 and α3β2, but not between α3β4 and α3β4α5 nAChRs

The decay of currents in response to 300 μM ACh (in the presence of 0.1 μM atropine) were fit to the sum of two exponential functions (see examples in Fig. 5C and Fig. 6D) with two time constants T_f (fast) and T_s (slow) and 3 amplitudes: A_f (fast), A_s (slow), and a plateau C. Note that time constants don't differ significantly between α3β4 and α3β4α5 receptors (in SCG neurons taken from α5β2 and β2 KO mice, respectively), whereas the relative contribution of A fast and A slow to the overall current differ slightly between the two genotypes ($P < 0.05$). In contrast, all parameters except of the cell capacitance ($P = 0.2480$, Student's *t*-test) differ significantly between α3β4 and α3β2 receptors ($P < 0.01$, Student's *t*-tests).

	α3β4 (n = 18)	**α3β4α5 (n = 18)**		**α3β4**	**α3β4α5**
A_f	13.0 ± 0.7 %[1]	16.8 ± 1.1 %[1]	T_f	444 ± 22 (msec)[2]	449 ± 30 (msec)[2]
A_s	56.3 ± 2.3 %[3]	48.6 ± 2.6 %[3]	T_s	5495 ± 496 (msec)[4]	5592 ± 509 (msec)[4]
C	30.5 ± 2.8 %[5]	34.5 ± 2.8 %[5]			
$A_f + A_s + C$	3747 ± 215 pA[6]	3907 ± 230 pA[6]			
Capacitance	49.1 ± 2.3 pF[7]	57.7 ± 3.6 pF[7]			

	α3β2 (n = 35)		
A_f	50.5 ± 2.1 %	T_f	132 ± 8 (msec)
A_s	36.2 ± 1.7 %	T_s	1129 ± 89 (msec)
C	13.2 ± 1.0 %		
$A_f + A_s + C$	1166 ± 77 pA		
Capacitance	54.1 ± 2.7 pF		

[1] A_f significantly different between α3β4 and α3β4α5 ($P = 0.0373$, Student's *t*-test)

[2] T_f not significantly different between α3β4 and α3β4α5 ($P = 0.8922$, Student's *t*-test)

[3] A_S significantly different between α3β4 and α3β4α5 ($P = 0.0119$, Student's *t*-test)

[4] T_S not significantly different between α3β4 and α3β4α5 ($P = 0.8887$, Student's *t*-test)

[5] C not significantly different between α3β4 and α3β4α5 ($P = 0.3323$, Student's *t*-test)

[6] Total amplitude not significantly different between α3β4 and α3β4α5 ($P = 0.6174$, Student's *t*-test)

[7] Capacitance not significantly different between α3β4 and α3β4α5 ($P = 0.0567$, Student's *t*-test)